2

Particle motion

2.1 Introduction

All microrheology experiments measure the resistance of a probe particle forced to move within a material, whether that probe is forced externally or simply allowed to fluctuate thermally. For example, the viscosity of a Newtonian liquid could be measured microrheologically, using a spherical colloid as a probe. In an active microrheology experiment, a colloid of radius a is driven externally with a specified force $\mathbf{F}$ (*e.g., magnetic, optical, or gravitational*), and moves with a velocity $\mathbf{V}$ that is measured. The rheology of the liquid (*i.e.*, the viscosity η) may be extracted from Stokes' classic formula for the drag on a sphere moving through a viscous fluid,

$$\zeta = \frac{F}{V} = 6\pi\eta a, \tag{2.1}$$

which will be computed in Section 2.5.2.

In passive microrheology experiments, on the other hand, the position of a thermally-fluctuating probe is tracked and analyzed to determine its diffusivity, which Einstein (1906) and Sutherland (1905) related to the hydrodynamic resistance ζ according to

$$D = \frac{k_B T}{\zeta} = \frac{k_B T}{6\pi\eta a}. \tag{2.2}$$

The interpretation of such experiments in purely viscous liquids is deceptively straightforward, as they rely upon hydrodynamic calculations by Stokes, Einstein, and Sutherland that are now taken for granted. To determine rheological properties (*e.g.*, G^*) from the probe resistance ζ in more complex materials, however, solutions to the analogous continuum-mechanics problem are required. Herein lies the difficulty: One must know the material's rheological properties in order to even pose the continuum-mechanical problem that must be solved, yet the solution of that problem is required to determine the material rheology! Fortunately, the Correspondence Principle (Section 2.4) cuts this Gordian Knot for linear response measurements. No such simplification occurs for nonlinear microrheology experiments, however, complicating their interpretation significantly.

Microrheology. Eric M. Furst and Todd M. Squires, Oxford University Press (2017).

DOI 10.1093/oso/9780199655205.001.0001

In this chapter, we briefly derive and discuss the fundamental equations governing continuum materials as they deform, and will specifically focus on the mechanics of probe particles moving within these materials.

2.2 The mechanics of deformable continua

Many readers are no doubt familiar with the Navier–Stokes equations, which govern the flow of viscous liquids. Some will also be familiar with the equations of motion for elastic solids. Both require the **continuum hypothesis**, which relies upon fictitious "material elements" that must satisfy two competing demands. Material elements must be large enough, and contain enough micro-structural elements (here atoms or molecules) to behave as the macro-scale material does. At the same time, material elements must be significantly smaller than any length scale associated with a flow or deformation field, so that gradients can be well-resolved.

The continuum approximation is easily satisfied with simple materials like water, glass, and steel on all but molecular length scales,

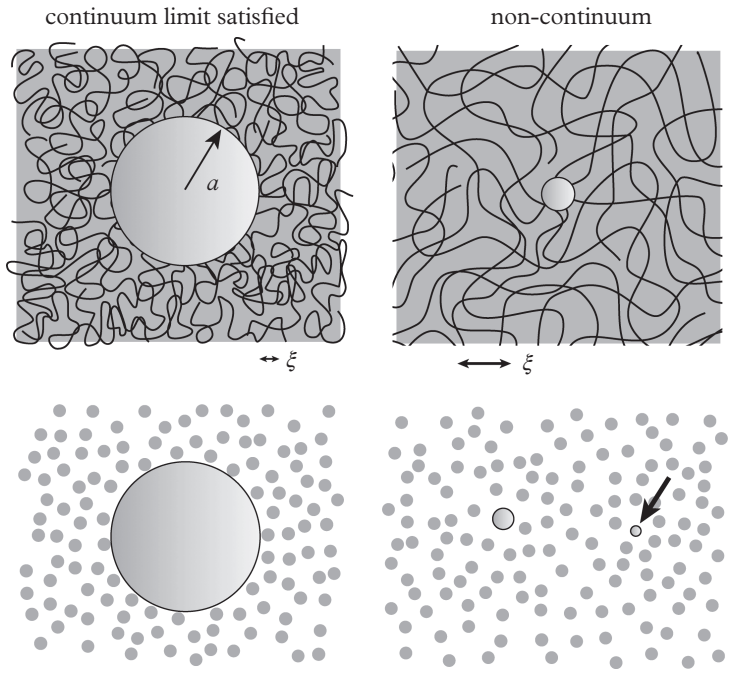

Fig. 2.1 *The continuum approximation is satisfied when probe particles are larger than the characteristic length scale ξ of the material. In materials like suspensions, the probe particle must be much larger than the dispersed particles. The arrow points to a probe that is smaller than the surrounding bath particles.*

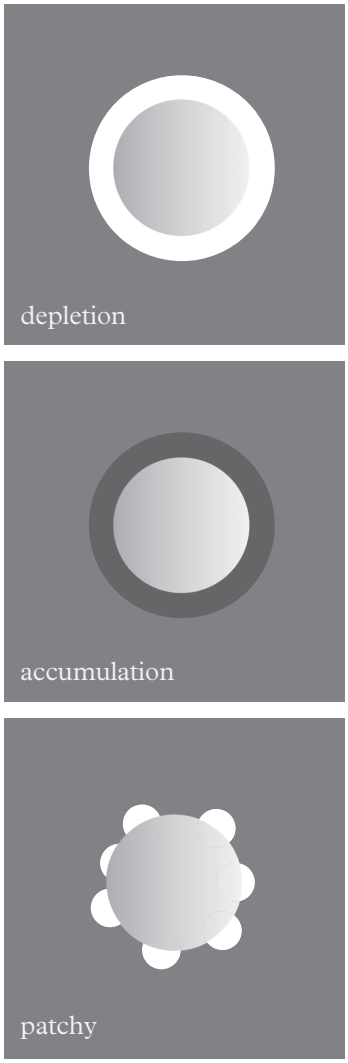

Fig. 2.2 *A second class of non-continuum effects occur in probe microrheology when the material structure is affected by the probe, in which case depleted layers, accumulation, or patchy interactions can arise.*

yet can be violated in microrheology of soft materials. For example, a grape embedded in Jello sees its material environment as a continuum: When forced, the grape deforms the surrounding Jello as a continuum. A sugar molecule or salt ion, however, is far smaller than the pores within the gel network comprising the Jello, and so diffuses through the Jello as though it were water. If this were a microrheology experiment, grape probes would (correctly) determine Jello to be a viscoelastic solid with the same $G^*(\omega)$ measured in a rheometer, whereas experiments using dye molecules as probes would reveal Jello to be a viscous liquid. Each experiment is meaningful in its own way—the grape correctly identifies the macroscopic rheology of Jello, whereas the dye reveals information about the mesostructure that would be inaccessible to macrorheometry. This example highlights both opportunities and challenges for the microrheologist.

Naturally, if a soft material has microstructural elements on the order of length scale ξ, then probe particles must exceed this dimension for the continuum approximation to hold. If the material contains dispersed polymers or particles, then those elements must be smaller than the probe. Both situations are represented in Fig. 2.1. An entangled biopolymer network, for instance, should have a mesh size $\xi \ll a$. Dispersed protein solutions, for which the individual molecules are on the order of tens of nanometers in size, naturally satisfy the continuum limit. But the microstructures in some gelators and rheology thickeners, including peptides, microgel particles, or clays, can often exceed normal probe dimensions of a few micrometers (Lu and Solomon, 2002; Oppong and de Bruyn, 2007; Savin and Doyle, 2007*a*; Rich *et al.*, 2011*b*). In Section 3.10, we discuss methods for verifying that the continuum approximation of probe microrheology is being met in an experiment. A second non-continuum effect occurs when the probe particle changes the local microstructure of the material. Material can be depleted near the particle, bunched up around it, or take on a more patchy structure, as we depict in Fig. 2.2. Later, we will discuss methods for detecting local heterogeneity, including manipulating the probe surface chemistry (Section 3.10), two-point microrheology experiments and the probe mechanics in locally heterogeneous materials (Section 4.11).

2.2.1 The Cauchy Stress Equation: $\mathbf{F} = M\mathbf{a}$ for continuum materials

When a material is treated as a continuum, rather than as some discrete object, Newton's equations must be "smeared out", with

masses and forces distributed on a per-volume basis. The Cauchy stress equation,[1]

$$\rho \frac{\partial^2 \mathbf{u}}{\partial t^2} = \nabla \cdot \boldsymbol{\sigma} + \mathbf{f}_b, \tag{2.3}$$

represents a continuum version of $\mathbf{F} = M\mathbf{a}$, which must be obeyed at each point $\mathbf{r}$ within the material. Note that ρ is the material density and $\mathbf{u}(\mathbf{r})$ represents the *displacement* of the material element at $\mathbf{r}$.

Three forces (per unit volume) appear in Eqn 2.3. The first term $\rho\ddot{\mathbf{u}}$ describes the inertial force density that arises at each point $\mathbf{r}$ within the material due to the unsteady acceleration of the material element. The third term, $\mathbf{f}_b$, represents a **body force** that is exerted throughout the volume of each material element. Common examples of body forces include gravitational, electrical, magnetic, and van der Waals forces. Unless otherwise noted, however, body forces will play little or no role in our discussion, and so will be omitted.

In Section 2.3, each material element accelerates due to **stresses** $\boldsymbol{\sigma}$ exerted on its surfaces by neighboring elements. The stress $\boldsymbol{\sigma}$ within a continuum material has units [force/area], and is a tensor quantity: The force $\mathbf{t}$ that is exerted per unit area of any particular surface depends on the orientation of that surface. The stress vector[2] exerted on a surface with outward-directed normal vector $\hat{\mathbf{n}}$ (Fig. 2.3) is given by

$$\mathbf{t} = \boldsymbol{\sigma} \cdot \hat{\mathbf{n}}, \tag{2.4}$$

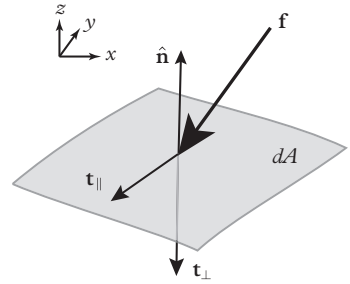

Fig. 2.3 *A force* $\boldsymbol{f}$ *exerted on an area segment dA with outward unit normal vector* $\hat{\boldsymbol{n}}$ *defines the stress vectors parallel* $\boldsymbol{t}_\parallel$ *and perpendicular* $\boldsymbol{t}_\perp$ *to the surface.*

and has components both normal to the surface (like pressure) and tangential to the surface (like viscous stresses). For example, the stress on a material located beneath $z = 0$, with outer normal $\hat{\mathbf{n}} = \hat{\mathbf{z}}$, is given by

$$\mathbf{t} = \sigma_{xz}\hat{\mathbf{x}} + \sigma_{yz}\hat{\mathbf{y}} + \sigma_{zz}\hat{\mathbf{z}}, \tag{2.5}$$

where, *e.g.*, $\sigma_{xz} = \hat{\mathbf{x}} \cdot \boldsymbol{\sigma} \cdot \hat{\mathbf{z}}$, and so on. σ_{xz} and σ_{yz} are shear stresses, and σ_{zz} is a normal stress.

The convective (nonlinear) derivative $\rho(\dot{\mathbf{u}} \cdot \nabla)\dot{\mathbf{u}}$ has been omitted from the left-hand side of eqn (2.3). As is familiar from fluid mechanics, two phenomena give rise to inertial forces. The first is the *unsteady* inertia $\rho\ddot{\mathbf{u}}$ that appears in (2.3). The other source arises even under steady flows (*i.e.*, when $\partial\mathbf{v}/\partial t = \ddot{\mathbf{u}} = 0$), when fluid elements are accelerated as they move along streamlines. The second (nonlinear) inertia gives rise to turbulence, whereas the first (linear) inertia gives rise to transverse waves. In microrheology, the *unsteady*

[1] Throughout this book, we will use lower-case variables $\mathbf{u}$ and $\mathbf{v} = \dot{\mathbf{u}}$ to represent displacement and velocity fields, respectively, within a continuum material. We will use upper-case variables $\mathbf{U}$ and $\mathbf{V}$ to denote the displacement and velocity of a particle within the material.

[2] Also called the traction.

inertia can be significant at high frequencies, but the *convective* inertia is generally not.

2.2.2 Linear-constitutive relations

The Cauchy Stress Equation (2.3) is exceedingly general, and governs the dynamics of all continuum materials—whether liquids, solids, gels, emulsions, solutions, powders, or foams. While powerful, it simply accounts for momentum conservation at every point in a material. To derive equations of motion for a particular material, we must know how the stress $\boldsymbol{\sigma}$ is related to the material's deformations: *e.g.*, strain (for elastic materials), strain-rate (for viscous materials), strain-rate history (for viscoelastic materials), metastable states (for powders and granular materials), and so on. These are **constitutive relations** and are specific to each material. Broad classes of constitutive relations distinguish between different classes of materials (*e.g.*, liquids versus solids), and material parameters within each constitutive relation distinguish between materials within each class (*e.g.*, viscosity for liquids, shear and bulk moduli for solids, and coefficients of restitution for granular materials).

The constitutive relation for a viscous liquid is particularly simple, and has proven remarkably successful. Other materials are not so simple, with stress tensors that are nonlinear functions of the strain and rate-of-strain tensors $\boldsymbol{\epsilon}$ and $\dot{\boldsymbol{\epsilon}}$, and of the deformation history of the material. Examples of rate-dependent responses include **shear thinning** in shampoo, and **shear thickening** in concentrated suspensions of cornstarch. Examples of strain-dependent responses include **strain hardening**: A rubber band pulls back gently when stretched slightly, but stiffens when stretched more. Some materials **yield**, like mayonnaise and toothpaste: They sit like elastic solids under gravitational stresses, yet flow like liquids under sufficiently large strains or stresses. Moreover, the stress in a material can depend on the type of deformation experienced by the material. Polymer solutions generally **shear thin**, such that they feel slippery, but **extension thicken** such that threads are hard to break. The constitutive relations for even simple elastic solids are generally only linear in the small-strain limits: Deform any solid significantly, and its response will change (*e.g.*, via ductile plasticity, or brittle fracture).

2.2.3 Constitutive relations in the linear response limit

Considerable simplifications arise in the **linear response** limit, which is found when deformations are so small or slow that the stress is simply proportional to the strain (or strain rate).

Viscous, or Newtonian, Liquids

Molecular liquids and gasses almost always operate in the linear response limit, as they are inherently disordered in a way that is not strongly disrupted by flow, except under exceptional circumstances, like appreciable Mach-number flows close to the speed of sound. When the fluids can be considered incompressible, $\nabla \cdot \mathbf{v} = 0$ must be imposed to conserve mass, and the stress is then given by

$$\boldsymbol{\sigma} = -p\boldsymbol{\delta} + 2\eta\dot{\boldsymbol{\epsilon}}, \tag{2.6}$$

where $\boldsymbol{\delta}$ is the identity tensor and

$$\dot{\boldsymbol{\epsilon}} = \frac{1}{2}\left(\nabla\dot{\mathbf{u}} + (\nabla\dot{\mathbf{u}})^T\right) \tag{2.7}$$

is the rate of deformation tensor. Equivalently, (2.7) can be expressed using index notation,

$$\dot{\epsilon}_{ij} = \frac{1}{2}\left(\frac{\partial \dot{u}_i}{\partial x_j} + \frac{\partial \dot{u}_j}{\partial x_i}\right), \tag{2.8}$$

and

$$\delta_{ij} = 1 \text{ for } i = j \tag{2.9}$$

$$\delta_{ij} = 0 \text{ for } i \neq j. \tag{2.10}$$

The stress in a viscous fluid depends only on the *rate* of deformation $\dot{\boldsymbol{\epsilon}}$ at a given time, rather than the total deformation $\boldsymbol{\epsilon}$ or any past history of deformation.

Compressible elastic solids

We will focus on elastic solids that are *isotropic*, as is appropriate for many soft materials. The conceptual differences that arise when treating anisotropic materials are relatively few, yet the mathematical complications are substantial, and would unnecessarily confuse the development of the core principles of microrheology presented here.[3] While viscous fluids are almost always incompressible, elastic materials often have a finite compressibility.

Two independent moduli are required to describe stress in isotropic elastic media—one for shear, and for compression. One way to write the stress in a compressible media is

$$\boldsymbol{\sigma} = \lambda(\nabla \cdot \mathbf{u})\boldsymbol{\delta} + 2G\boldsymbol{\epsilon}, \tag{2.11}$$

[3] Anisotropic-elastic solids (*e.g.*, crystals) generally require a fourth-rank stiffness tensor $\mathbf{C}$ for their description, $\boldsymbol{\sigma} = \mathbf{C} : \boldsymbol{\epsilon}$, or $T_{ij} = C_{ijkl}\epsilon_{kl}$.

wherein λ is Lamé's first coefficient, which involves material compressibility, and G is the standard shear modulus. Although this form of the stress tensor is the simplest to write, it is not necessarily the clearest form conceptually, in terms of differentiating between shear and compressive properties. To see this, note that the trace of $\boldsymbol{\epsilon}$ is $\nabla \cdot \mathbf{u}$, which is not necessarily zero in compressible media. Consequently, the stress arising from compressive deformations includes contributions from both the shear modulus G and λ. Specifically, the (isotropic) stress in response to a pure compressive strain is given by

$$\sigma_{ii} = (3\lambda + 2G)\nabla \cdot \mathbf{u}. \tag{2.12}$$

Thus, it is often convenient to explicitly define a bulk modulus K,

$$K = \lambda + \frac{2}{3}G, \tag{2.13}$$

so that

$$\sigma_{ii} = 3K\nabla \cdot \mathbf{u}. \tag{2.14}$$

When written in terms of the bulk and shear moduli K and G, the stress tensor explicitly separates into two components: One associated with volume-preserving deformations, and the other with compressive deformations:

$$\boldsymbol{\sigma} = K(\nabla \cdot \mathbf{u})\boldsymbol{\delta} + 2G\left(\boldsymbol{\epsilon} - \frac{1}{3}(\nabla \cdot \mathbf{u})\boldsymbol{\delta}\right). \tag{2.15}$$

Various choices are thus available to describe isotropic, compressible media. We have seen three: The shear modulus G, the bulk modulus K, and Lamé's first coefficient λ. Another common choice is the Poisson ratio ν, which gives the ratio of how much a material *expands* in a direction *transverse* to the direction in which it is compressed. An incompressible material, for example, has $\nu = 1/2$: If compressed with a strain Δ in the z-direction, it must expand with strains $\Delta/2$ in the x and y directions to preserve volume. The Poisson ratio can be derived from the shear and bulk moduli according to

$$\nu = \frac{3K - 2G}{2(3K + G)}, \tag{2.16}$$

giving a stress tensor of the form

$$\boldsymbol{\sigma} = G\left[\frac{2\nu}{1 - 2\nu}(\nabla \cdot \mathbf{u})\boldsymbol{\delta} + 2\boldsymbol{\epsilon}\right]. \tag{2.17}$$

The final two moduli in common use are Young's modulus E, which relates uniaxial strain (stretching) to unaxial stress, and the P-wave or longitudinal modulus, which describes axial stress in response to strains that are *purely* axial (*e.g.*, as occurs in pressure (P) waves).

To summarize, two independent moduli are required to describe the stress-strain relationship in compressible, isotropic media. There are six such moduli in common use, every one of which can be expressed in terms of two others, giving 15 superficially distinct expressions for $\boldsymbol{\sigma}$. Any of these expressions (*i.e.*, any pair of moduli) can be used to pose and solve a given elasticity problem. Which pair is best depends on the natural geometry of the problem and to a large extent on one's taste.

In rheology and microrheology, the shear modulus G is almost always the property of interest, and so will be retained throughout this text. Various choices are often chosen for the second modulus—usually λ, K or ν. We will generally present results in terms of G and K.

Incompressible elastic solids

Some elastic materials (*e.g.*, Jello) are much harder to compress than to shear, and can often be approximated as *incompressible*. This occurs when the bulk modulus K is much larger than the shear modulus G, so that deformations with non-zero divergence $\nabla \cdot \mathbf{u}$ would give rise to stresses $K\nabla \cdot \mathbf{u}$ that are enormous compared to shear stresses $\sim G\nabla\mathbf{u}$.

Approximating a material as incompressible is mathematically subtle, requiring the limit $K \to \infty$ to be taken while simultaneously imposing $\nabla \cdot \mathbf{u} \to 0$. It is not immediately obvious whether the compressive stress $-K\nabla \cdot \mathbf{u}$ should be infinity, or zero, or something finite. The standard approach, familiar in fluid mechanics, is to define a pressure $p = -K(\nabla \cdot \mathbf{u})$ as a separate field whose function is to enforce the incompressibility condition $\nabla \cdot \mathbf{u} = 0$, which is imposed as a separate equation. In this case, the linear response constitutive equations for an isotropic, incompressible elastic solid are given by

$$\boldsymbol{\sigma} = -p\boldsymbol{\delta} + 2G\boldsymbol{\epsilon}. \tag{2.18}$$

$$\nabla \cdot \mathbf{u} = \mathrm{Tr}\,\boldsymbol{\epsilon} = 0. \tag{2.19}$$

Notably, this constitutive relation is identical in form to that for an incompressible viscous liquid (eqn 2.6), but depends on strain $\boldsymbol{\epsilon}$ rather than rate of strain $\dot{\boldsymbol{\epsilon}}$.

Incompressible, isotropic viscoelastic materials

Finally, we turn to linear viscoelastic (LVE) materials, which exhibit both viscous and elastic responses to deformations. LVE materials

have frequency-dependent moduli, reflecting the relaxation of different structural modes that occur at different time scales. We will focus on incompressible LVE materials, since most soft materials consist of some meso-structure suspended in a viscous liquid, and viscous liquids are essentially always treated as incompressible.

When an LVE material is subjected to a gentle oscillatory deformation

$$\boldsymbol{\epsilon}(t;\omega) = \boldsymbol{\epsilon}_0 e^{i\omega t}, \tag{2.20}$$

at frequency ω, the resulting stress,

$$\boldsymbol{\sigma}(t;\omega) = \boldsymbol{\sigma}_0 e^{i(\omega t+\delta)}, \tag{2.21}$$

need not be in-phase with the strain. Instead, the stress is given by

$$\boldsymbol{\sigma}_0(\omega) = -p_0(\omega)\boldsymbol{\delta} + G^*(\omega)\boldsymbol{\epsilon}_0(\omega), \tag{2.22}$$

where

$$G^*(\omega) = G_0 e^{i\delta} \tag{2.23}$$

is the complex-storage modulus, and δ is the phase angle between shear stress and shear strain. The phase angle δ is zero for elastic solids, where stress and strain are in phase, and is $\delta = \pi/2$ for viscous liquids, for which the stress is in-phase with the strain rate.[4]

Under linear response conditions, the stress tensor $\boldsymbol{\sigma}(t)$ in a linear viscoelastic liquid at any time t due to a general (but gentle) strain history,

$$\boldsymbol{\epsilon}(t) = \frac{1}{2\pi}\int_{-\infty}^{\infty} \tilde{\boldsymbol{\epsilon}}(\omega) e^{i\omega t} d\omega, \tag{2.24}$$

is then simply given by superposing the responses at each frequency, with the appropriate amplitude:

$$\boldsymbol{\sigma}(t) = \frac{1}{2\pi}\int_{-\infty}^{\infty} \left[-\tilde{p}(\omega)\boldsymbol{\delta} + G^*(\omega)\tilde{\boldsymbol{\epsilon}}(\omega)\right] e^{i\omega t} d\omega, \tag{2.25}$$

giving

$$\boldsymbol{\sigma}(t) = -p(t)\boldsymbol{\delta} + \int_{-\infty}^{t} m(t-t')\boldsymbol{\epsilon}(t')dt'. \tag{2.26}$$

Here $m(t)$ is the **memory function**, defined by

$$m(t) = \frac{1}{2\pi}\int_{-\infty}^{\infty} G^*(\omega) e^{i\omega t} d\omega. \tag{2.27}$$

Notably, eqn 2.27 reveals that the stress at time t depends upon the strain history at previous times $t' < t$, weighted by the memory function $m(t)$.

[4] Note that some authors use $e^{-i\omega t}$ rather than $e^{i\omega t}$ in defining viscoelastic materials. Both are equivalent, although it is common for confusion and errors to arise when results from both conventions are used.

2.3 Equations of motion for isotropic continua

It is now straightforward to derive equations of motion for various materials by simply evaluating the Cauchy Stress equation (2.3) using the relevant constitutive equation for each material.

We start with incompressible materials, which obey

$$\nabla \cdot \dot{\mathbf{u}} = \nabla \cdot \mathbf{u} = 0. \tag{2.28}$$

The momentum equations differ from material to material, and are given by

$$\rho \ddot{\mathbf{u}} = -\nabla p + \eta \nabla^2 \dot{\mathbf{u}} \tag{2.29}$$

for incompressible viscous liquids,

$$\rho \ddot{\mathbf{u}} = -\nabla p + G \nabla^2 \mathbf{u} \tag{2.30}$$

for isotropic, incompressible elastic solids, and

$$\rho \ddot{\mathbf{u}} = -\nabla p + \int_{-\infty}^{t} m(t - t') \nabla^2 \mathbf{u}(t') dt' \tag{2.31}$$

for isotropic, incompressible viscoelastic media.

Equations (2.29) and (2.30) for (incompressible) viscous liquids and elastic solids appear quite similar, differing by one mere time derivative. The momentum equation for an incompressible, isotropic-viscoelastic material (eqn 2.31) at first glance appears quite different. However, computing the Fourier time-transforms of eqns 2.29–2.31 yields

$$-\rho \omega^2 \tilde{\mathbf{u}} = -\nabla \tilde{p} + i\omega\eta \nabla^2 \tilde{\mathbf{u}} \tag{2.32}$$

$$-\rho \omega^2 \tilde{\mathbf{u}} = -\nabla \tilde{p} + G \nabla^2 \tilde{\mathbf{u}} \tag{2.33}$$

$$-\rho \omega^2 \tilde{\mathbf{u}} = -\nabla \tilde{p} + G^*(\omega) \nabla^2 \tilde{\mathbf{u}}. \tag{2.34}$$

Remarkably, the momentum equations for viscous fluids, elastic solids, and viscoelastic materials are essentially identical. These equations differ only in their scalar shear moduli, which are purely imaginary ($i\omega\eta$) for liquids (eqn 2.32), purely real (G) for solids (eqn 2.33), and generally complex $G^*(\omega)$ for viscoelastic materials (eqn 2.34). Moreover, stress tensors for all three transform similarly:

$$\tilde{\boldsymbol{\sigma}} = -\tilde{p}(\omega)\boldsymbol{\delta} + G^*(\omega)\tilde{\boldsymbol{\epsilon}}, \tag{2.35}$$

where $G^*(\omega)$ can now be viewed as a general shear modulus: $G^*(\omega) = i\omega\eta$ for a purely viscous liquid, and $G^*(\omega) = G$ for a purely elastic solid.

These equations can equally well be expressed in terms of velocity fields $\tilde{\mathbf{v}} = i\omega\tilde{\mathbf{u}}$, in which case eqn 2.34 becomes

$$i\rho\omega\tilde{\mathbf{v}} = -\nabla\tilde{p} + \eta^*(\omega)\nabla^2\tilde{\mathbf{v}}. \tag{2.36}$$

When writing equations of motion in terms of velocity fields $\tilde{\mathbf{v}}$, rather than displacement fields $\tilde{\mathbf{u}}$, it is often sensible to introduce the **complex viscosity**

$$\eta^*(\omega) \equiv \frac{G^*(\omega)}{i\omega}, \tag{2.37}$$

rather than the shear modulus $G^*(\omega)$. Both approaches are valid, and are entirely equivalent, although $G^*(\omega)$ can can only be determined from $\eta^*(\omega)$ to within a single, additive constant, typically $G'(\omega \to 0)$.

Analogous results hold when the Laplace transform is employed, rather than the Fourier Transform, although subtleties exist regarding initial conditions, since Laplace Transforms single out a particular $t = 0$. For simplicity's sake, we will assume homogeneous initial conditions: $\mathbf{u}(t \leq 0) = \dot{\mathbf{u}}(t \leq 0) = \mathbf{0}$. In that case, the Laplace-Transformed equations of motion for viscous fluids, elastic solids, and viscoelastic media become

$$\rho s^2\hat{\mathbf{u}} = -\nabla\hat{p} + s\eta\nabla^2\hat{\mathbf{u}} \tag{2.38}$$

$$\rho s^2\hat{\mathbf{u}} = -\nabla\hat{p} + G\nabla^2\hat{\mathbf{u}} \tag{2.39}$$

$$\rho s^2\hat{\mathbf{u}} = -\nabla\hat{p} + \hat{G}(s)\nabla^2\hat{\mathbf{u}}. \tag{2.40}$$

or, using velocity rather than displacement fields,

$$\rho s\hat{\mathbf{v}} = -\nabla\hat{p} + \hat{\eta}(s)\nabla^2\hat{\mathbf{v}}, \tag{2.41}$$

where

$$\hat{\eta}(s) = \hat{G}(s)/s \tag{2.42}$$

is the Laplace-Transformed complex viscosity.

Equations (2.32–2.41) have profound implications for microrheology, as developed in Section 2.4.

2.4 Correspondence Principle

A remarkable feature of the time-transformed equations of motion for isotropic and incompressible materials—given by eqns 2.32–2.34—is that they are essentially identical, no matter whether the material is a viscous liquid, an elastic solid, or more generally viscoelastic. All such materials obey the same time-transformed equations of motion, with a shear modulus $G^*(\omega)$ that would be purely imaginary for a viscous liquid, purely real for an elastic solid, or complex for a viscoelastic material.

This observation forms the basis for the **Correspondence Principle** (Pipkin, 1986), which provides a simple way to solve linear viscoelastic flow or displacement problems, by simply adapting a solution to a corresponding Stokes flow or elastisity problem. Its traditional formulation holds for viscoelastic materials that

- can be treated as **continuum**;
- are spatially **homogeneous**;
- are spatially **isotropic**;
- can be approximated as **incompressible**; and
- are deformed gently enough that the **linear response** approach remains valid.

Correpondence Principle: Time-transformed LVE flows can be obtained from analogous solutions to the Stokes flow or elasticity equations, by replacing the Newtonian viscosity η is replaced by the complex viscosity $\eta^*(\omega)$, or elastic shear modulus G by the complex shear modulus $G^*(\omega)$.

The time-transformed equations of motion for LVE materials (eqn 2.34) are identical to the time-transformed Stokes equations (eqn 2.32) for viscous flow when η is replaced by $\eta^*(\omega)$. One can therefore take a time-transformed solution $\mathbf{v}_{\text{Stokes}}$ to a Stokes flow problem with a given geometry, and replace the Stokes viscosity η with a complex viscosity $\eta^*(\omega)$, to obtain a valid time-transformed solution to the corresponding problem for an LVE material with complex viscosity $\eta^*(\omega)$,

$$\tilde{\mathbf{v}}_{\text{LVE}}(\omega) = \tilde{\mathbf{v}}_{\text{Stokes}}(\omega)\big|_{\eta \to \eta^*(\omega)}\,, \tag{2.43}$$

so long as the time-transformed boundary conditions of the LVE problem are also identical to those of the time-transformed Stokes flow problem. Similarly, one can take a time-transformed displacement field $\mathbf{u}_{\text{Elasticity}}$ computed for an incompressible solid, and replace the shear modulus G with the complex shear modulus $G^*(\omega)$, to obtain a valid time-transformed LVE displacement field $\tilde{\mathbf{u}}_{\text{LVE}}(\omega)$,

$$\tilde{\mathbf{u}}_{\text{LVE}}(\omega) = \tilde{\mathbf{u}}_{\text{Elasticity}}(\omega)\big|_{G \to G^*(\omega)}\,. \tag{2.44}$$

Analogous results hold for Laplace-Transformed fields.

Consider the example of a plate at $z = 0$ executing transverse oscillations of amplitude U_0 and frequency ω. The plate excites elastic shear waves that propagate through an elastic medium, giving a displacement field

$$u_x(z) = \mathrm{Re}\left(U_0 e^{i\omega(t-z/c)}\right) = U_0 \cos\left[\omega\left(\frac{z}{c} - t\right)\right], \tag{2.45}$$

where

$$c = \sqrt{G/\rho} \tag{2.46}$$

is the transverse wave speed in the medium. An alternative form,

$$u_x(z) = \mathrm{Re}\left(U_0 e^{i(\omega t - q_T z)}\right) = U_0 \cos\left[q_T z - \omega t\right], \tag{2.47}$$

highlights the transverse-wave number,

$$q_T = \frac{2\pi}{\lambda_T} = \sqrt{\frac{\rho\omega^2}{G}}. \tag{2.48}$$

Direct substitution confirms that eqns 2.45 and 2.47 obey eqn 2.33.

The analogous problem for a viscous fluid—where a plate at $z = 0$ oscillates in the x-direction with amplitude U_0 and frequency ω—can be obtained directly from eqn 2.45 using the Correspondence Principle. Replacing the elastic shear modulus G in eqn 2.47 with the modulus for a viscous fluid ($G \to i\omega\eta$) gives

$$-iq_T z \to -iz\sqrt{\frac{\rho\omega^2}{i\omega\eta}} = \pm(i+1)\frac{z}{\lambda_V}, \tag{2.49}$$

where we have used $\sqrt{i} = \pm(1+i)/\sqrt{2}$, and where

$$\lambda_V = \sqrt{\frac{2\eta}{\rho\omega}} = \sqrt{\frac{2\nu}{\omega}} \tag{2.50}$$

is the oscillatory boundary layer thickness. The displacement field for a *Stokes* flow, obtained from eqn 2.45 using the Correspondence Principle, is then

$$u_x(z) \to \mathrm{Re}\left[U_0 \exp\left(i\omega t \pm (i+1)\frac{z}{\lambda_V}\right)\right]. \tag{2.51}$$

Choosing the negative root ensures the displacement field decays as $z \to \infty$, giving

$$u_x(z) = U_0 \cos\left(\omega t - \frac{z}{\lambda_V}\right) e^{-z/\lambda_V}. \tag{2.52}$$

The *flow* field $\mathbf{v}$ follows from the *displacement* field $\mathbf{u}$ via $\mathbf{v} = i\omega\mathbf{u}$, giving the expected oscillatory boundary layer velocity field

$$v_x(z) = V_0 \cos\left(\omega t - \frac{z}{\lambda_V}\right) e^{-z/\lambda_V} \tag{2.53}$$

in terms of the velocity V_0 of the oscillating plate.

Solutions for shear waves in LVE materials may be obtained similarly, using a complex modulus,

$$G^*(\omega) = G_0 e^{i\delta}, \tag{2.54}$$

giving

$$u_x(z) = U_0 \cos\left(\omega t - q_T^* z\right) e^{-z/\lambda_V^*}, \tag{2.55}$$

with wavenumber q_T^*,

$$q_T^* = \sqrt{\frac{\rho\omega^2}{G_0}} \cos\frac{\delta}{2} \tag{2.56}$$

and attenuation length λ_V^*,

$$\lambda_V^* = \sqrt{\frac{G_0}{\rho\omega^2}} \frac{1}{\sin\frac{\delta}{2}}. \tag{2.57}$$

Equations 2.55–2.57 recover elastic shear waves (eqn 2.45) in the $\delta \to 0$ limit appropriate for pure elastic materials, and viscous shear waves (eqns 2.50 and 2.52) in the $\delta \to \pi/2$ limit relevant for viscous fluids. For all linear viscoelastic materials (with phase angles $0 \leq \delta < \pi/2$), the thickness λ_V^* of the oscillatory-boundary layer exceeds the wavelength λ_V of the oscillatory shear waves, becoming equal only in the purely viscous limit $\delta = \pi/2$. These shear waves are depicted in Fig. 2.4.

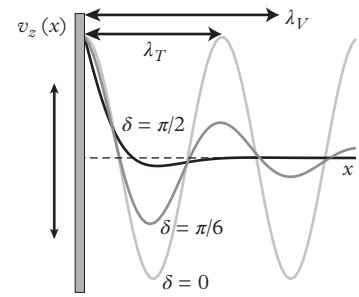

Fig. 2.4 *Shear waves near an oscillating plate for viscous, elastic, and viscoelastic materials.*

2.5 Particle motion

Earlier, we posed an apparent conundrum central to microrheology: In order to infer the material rheology from measurements of a probe's response, one must solve a continuum-mechanics problem. In order to even pose this continuum-mechanical problem in the first place, however, one must know the material rheology! As we shall shortly see the Correspondence Principle circumvents this difficulty. So long as material's constitutive equations are consistent with the Correspondence Principle, one can simply take solutions to the viscous-flow (or elastic displacement) field around the force probe, and replace the Newtonian viscosity with the corresponding complex viscosity appropriate for the material. The Correspondence Principle, then, paves the way for the widespread success of microrheology.

We therefore turn to the continuum-mechanics of particle motion.

2.5.1 Mobility and resistance

We start by discussing the hydrodynamic **resistance** ζ of a probe forced to move within a liquid, as well as its **mobility** b. In a Newtonian liquid, the mobility and resistance are *linear response* properties. The resistance ζ gives the drag force $\mathbf{F}_d$ on a probe translating with velocity $\mathbf{V}$ through the liquid, whereas the mobility b gives the probe velocity $\mathbf{V}$ in response to a driving force $\mathbf{F}$:

$$\mathbf{F}_d = -\zeta \mathbf{V}, \quad \mathbf{V} = b\mathbf{F}. \tag{2.58}$$

We have assumed a spatially isotropic probe, for which ζ and b are scalar quantities; more generally, mobility and resistance *tensors* are required for anisotropic particles, as explored in Section 2.8.

The mobility and resistance of probes take more complex forms in viscoelastic media,

$$\mathbf{F}_d(t) = -\int_{-\infty}^{t} \zeta(t-t')\mathbf{V}(t')dt' \tag{2.59}$$

$$\mathbf{V}(t) = \int_{-\infty}^{t} b(t-t')\mathbf{F}(t')dt'. \tag{2.60}$$

meaning that the velocity of a probe depends on its past force history, and vice versa. The mobility and resistance are thus not simple inverses of each other, as they are for Newtonian fluids (cf. eqn 2.58). Their time-transformed versions, however, are:

$$\tilde{\mathbf{F}}_d(\omega) = -\zeta^*(\omega)\tilde{\mathbf{V}}(\omega) \tag{2.61}$$

$$\tilde{\mathbf{V}}(\omega) = b^*(\omega)\tilde{\mathbf{F}}(\omega), \tag{2.62}$$

from which it follows that, for $\mathbf{F}_d = -\mathbf{F}$,

$$\zeta^*(\omega)b^*(\omega) = 1. \tag{2.63}$$

These equations are central to understanding the response of probe particles to applied or inherent (thermal) forces. On a practical level, it is often easier to pose the resistance problem than the mobility problem if one needs to compute these quantities (*e.g.*, for a complex probe shape, or in a complex geometry). This is because the resistance problem involves a standard boundary condition, in which the *velocity* is specified on every point of the probe surface. By contrast, the mobility problem imposes the *total* force (and torque) on the particle, without specifying how the stress is distributed over the probe surface.

While it is more natural to solve the resistance problem, and then invert the resistance to obtain the mobility, this inversion can be subtle. As discussed in Sections 2.6.2 and 2.8, anisotropic and multiparticle systems generally have tensor mobilities and resistances, for which one cannot simply invert one component (*e.g.*, ζ_{xx}) of the resistance tensor to obtain that component (b_{xx}) of the mobility tensor. Rather, the full-resistance tensor must be inverted to obtain the mobility tensor.

Lastly, in keeping with the concept of the Correspondence Principle, the mobility and resistance relations between the force on a probe and its velocity may alternately be expressed in the form of a spring constant (possibly complex) that relates the displacement to the force:

$$\mathbf{F}(t) = -\int_{-\infty}^{t} \kappa(t-t')\mathbf{U}(t')dt', \tag{2.64}$$

which when Fourier transformed becomes

$$\tilde{\mathbf{F}}(\omega) = -\tilde{\kappa}^*(\omega)\tilde{\mathbf{U}}(\omega). \tag{2.65}$$

Since $\tilde{\mathbf{F}} = i\omega\tilde{\mathbf{U}}$, the complex spring constant is related to the complex resistance via

$$\tilde{\kappa}^*(\omega) = i\omega\tilde{\zeta}^*(\omega). \tag{2.66}$$

2.5.2 The Stokes resistance and mobility of a translating sphere

We start with the simplest, most well-known, and most important example—the Stokes resistance of a solid sphere of radius a, centered at $\mathbf{r} = \mathbf{0}$ and translating with velocity $\mathbf{V}_0$ in a fluid of viscosity η. The

fluid is set into motion, with velocity, pressure, and stress fields given by $\{\mathbf{v}, p, \boldsymbol{\sigma}\}$. The Stokes equations 2.29 are solved subject to no-slip boundary conditions on the sphere surface ($\mathbf{v} = \mathbf{V}_0$ for $r = a$) and no-disturbance far away ($\mathbf{v} \to 0$ as $r \to \infty$). The stream function,

$$\psi(\mathbf{r}, \theta) = \left(\frac{3r}{2a} - \frac{a}{2r}\right) \frac{a^2 \sin^2\theta}{2} V_0, \tag{2.67}$$

gives a compact form of the solution as a function of position $\mathbf{r}$ around the translating sphere, from which the velocity fields are obtained via

$$v_r = \frac{1}{r^2 \sin\theta} \frac{\partial \Psi}{\partial \theta} \tag{2.68}$$

$$v_\theta = -\frac{1}{r \sin\theta} \frac{\partial \Psi}{\partial r}. \tag{2.69}$$

The velocity and pressure fields around a sphere translating with velocity $\mathbf{V}_0$ are then given by[5]

$$\mathbf{v}(\mathbf{r}) = \frac{3a}{4r}\left(\mathbf{V}_0 + (\mathbf{V}_0 \cdot \hat{\mathbf{r}})\hat{\mathbf{r}}\right) + \frac{a^3}{4r^3}\left(\mathbf{V}_0 - 3(\mathbf{V}_0 \cdot \hat{\mathbf{r}})\hat{\mathbf{r}}\right) \tag{2.70}$$

$$p(\mathbf{r}) = \frac{3\eta}{2a}\frac{a^2}{r^2}\mathbf{V}_0 \cdot \hat{\mathbf{r}} \tag{2.71}$$

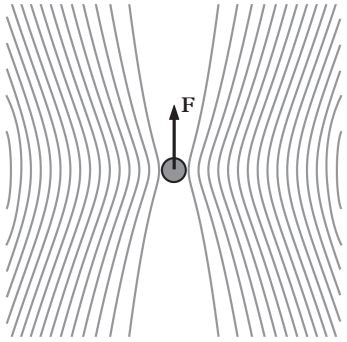

Fig. 2.5 *Flow generated by a translating sphere. In a fixed reference frame, the fluid flow around a sphere consists of a Stokeslet (Fig. 2.7) and Source Dipole (Fig. 2.8). At long distances, the Stokeslet flow field dominates, which decays with distance like* r^{-1}.

and stress tensor

$$\boldsymbol{\sigma}(\mathbf{r}) = -\frac{9\eta a}{2r^2}\mathbf{V}_0 \cdot \hat{\mathbf{r}}\hat{\mathbf{r}}\hat{\mathbf{r}} + \frac{3\eta a^3}{2r^4}\left(5\mathbf{V}_0 \cdot \hat{\mathbf{r}}\hat{\mathbf{r}}\hat{\mathbf{r}} - \hat{\mathbf{r}}\mathbf{V}_0 - \mathbf{V}_0\hat{\mathbf{r}} - \mathbf{V}_0 \cdot \hat{\mathbf{r}}\boldsymbol{\delta}\right) \tag{2.72}$$

where

$$\hat{\mathbf{r}} = \frac{\mathbf{r}}{r} \tag{2.73}$$

is the unit vector in the radial direction. The velocity field in a fixed-reference frame and in the reference frame of the translating probe are shown in Fig. 2.5 and Fig. 2.6, respectively. The fixed-reference frame will be useful later when we consider the interactions between neighboring particles, while the sphere's reference frame provides a sense of the mix of deformation modes (*e.g.*, shear *versus* extension) and Lagrangian unsteadiness material elements experience as they move around it.

[5] In Appendix A.4 we use a vector-harmonic functions to arrive at the same solution.

Finally, we compute the force $\mathbf{F}_0$ exerted by the fluid on the particle via

$$\mathbf{F}_0 = \int_{r=a} \hat{\mathbf{r}} \cdot \boldsymbol{\sigma}\, dA = 6\pi\eta a \mathbf{V}_0, \tag{2.74}$$

revealing the hydrodynamic resistance ζ_T^{sphere} of a translating sphere to be given by

$$\zeta_T^{\text{sphere}} = 6\pi\eta a. \tag{2.75}$$

The mobility b_T^{sphere} of a translating sphere can now be easily determined by simply inverting ζ_T^{sphere} (eqn 2.75),

$$b_T^{\text{sphere}} = \frac{1}{6\pi\eta a}. \tag{2.76}$$

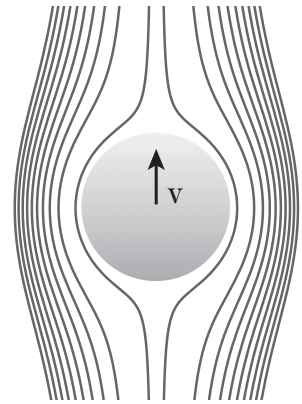

Fig. 2.6 *Streamlines in the reference frame of the translating sphere highlight the material deformation.*

The translation of viscous liquid drops and gas bubbles can be treated in a similar fashion, with the no-slip boundary condition replaced by the relevant stress-matching boundary condition. The translation of a liquid drop is described by the Hadamard–Rybczinski formula,

$$\zeta_T^{\text{drop}} = 4\pi\eta a \frac{3\lambda_\eta + 2}{2(\lambda_\eta + 1)} \tag{2.77}$$

where $\lambda_\eta = \eta_d/\eta$ is the viscosity ratio of the drop to that of the surrounding medium. As $\lambda_\eta \to \infty$, the Stokes resistance of a rigid sphere is recovered,

$$\zeta(\lambda_\eta \to \infty) \to 6\pi\eta a. \tag{2.78}$$

The limit $\lambda_\eta \to 0$, corresponding to an inviscid bubble, gives a resistance

$$\zeta(\lambda_\eta \to \infty) \to 4\pi\eta a \tag{2.79}$$

that is lower than for the rigid sphere, but only by 50%.

The fluid velocity field (eqn 2.70) naturally splits into two distinct components: The first term decays slowly ($\sim r^{-1}$) and represents the flow due to a point force, or **Stokeslet**, at the origin. The Stokeslet flow gives rise to the slowest-decaying (r^{-2}) first term in eqn 2.72, and is entirely responsible for the drag on the sphere, as shown in Fig. 2.7 and Fig. 2.8. The second term in the flow field decays more quickly ($\sim r^{-3}$) and represents a potential dipole, or "point source" dipole.

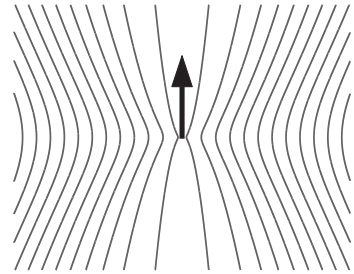

Fig. 2.7 ***Stokeslet*** *flow field. The fluid flow established by a point force, called a Stokeslet, decays like* $1/r$.

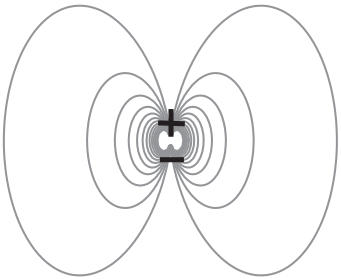

Fig. 2.8 ***Potential*** *dipole field. The fluid flow established by a point-source dipole decays like* $1/r^3$.

The source dipole flow is irrotational, and gives rise to the second ($\sim r^{-4}$) term in the stress tensor (2.72) and does not contribute to the drag. Equation 2.70 can be written

$$\mathbf{v}(\mathbf{r}) = 6\pi\eta a \left(\mathbf{G}^{\mathrm{St}}(\mathbf{r}) - \frac{a^2}{3}\mathbf{G}^{\mathrm{PD}}(\mathbf{r}) \right) \cdot \mathbf{V}_0, \tag{2.80}$$

$$= \left(\mathbf{G}^{\mathrm{St}}(\mathbf{r}) - \frac{a^2}{3}\mathbf{G}^{\mathrm{PD}}(\mathbf{r}) \right) \cdot \mathbf{F}_0, \tag{2.81}$$

where $\mathbf{G}^{\mathrm{St}}(\mathbf{r})$ and $\mathbf{G}^{\mathrm{PD}}(\mathbf{r})$ represent the Green's functions for a point force and a (potential) source dipole, respectively, located at the origin:

$$\mathbf{G}^{\mathrm{St}}(\mathbf{r}) = \frac{1}{8\pi\eta}\left(\frac{\boldsymbol{\delta}}{r} + \frac{\hat{\mathbf{r}}\hat{\mathbf{r}}}{r} \right), \tag{2.82}$$

$$\mathbf{G}^{\mathrm{PD}}(\mathbf{r}) = \frac{1}{8\pi\eta}\left(-\frac{\boldsymbol{\delta}}{r^3} + 3\frac{\hat{\mathbf{r}}\hat{\mathbf{r}}}{r^3} \right) \equiv \frac{1}{8\pi\eta}\nabla\nabla\left(\frac{1}{r} \right). \tag{2.83}$$

The Stokeslet tensor $\mathbf{G}^{\mathrm{St}}$ is also known as the **Oseen tensor**. The flow field at large distances r from the probe is dominated by the Stokeslet flow, which depends only on the total force, rather than the size (or even shape) of the particle. The second (potential) component decays more quickly, and is shape-dependent.

The flow around a translating sphere is special in that exactly two terms ($\mathbf{G}^{\mathrm{St}}$ and $\mathbf{G}^{\mathrm{PD}}$) are required for its description. An infinite number of terms (comprised of all multipoles of point forces and sources) are generally required to describe the flow around more general shapes. Several key features are preserved even for complex-shaped probes, however. The Stokeslet flow $\mathbf{G}^{\mathrm{St}}$ depends only upon the force on the probe, and represents the only component of the flow that decays with distance like r^{-1}.

The higher-order multipoles depend on the detailed probe shape, and are essential in determing the self-mobility and self-resistance of the probe. Hydrodynamic interactions between well-separated particles, on the other hand, are dominated by the slowest-decaying components of the flow, as discussed in Section 2.6. The "coupling mobilities" between particles, then, are dominated by the Stokeslet flow. This motivates *two-point* microrheology techniques (see Section 4.11), which measure the cross-correlated fluctuations of two different probes. These cross correlations are proportional to the *coupling mobility* (which gives the velocity of one particle in response to a force on the other particle), which depends almost exclusively on the Stokeslet term, and is therefore essentially independent of the shape of each probe.

2.5.3 Stokes resistance of a probe undergoing oscillatory translations

Thus far, we have examined *steady* probe motion. Diffusing particles, by contrast, execute stochastic, fluctuating motions, which can be decomposed (through the Fourier Transform) to oscillatory motions at every frequency. Oscillations at sufficiently low frequencies are well-described by the steady Stokes flow solutions computed (*i.e.*, the *quasi-steady* approximation). Above a characteristic inertial frequency, however, the response of a sphere to an oscillatory force changes qualitatively, significantly impacting the interpretation of a microrheology experiment. One thus needs to know the relevant frequency where fluid inertia (and thus transient flow behavior) becomes important, and how this frequency scales with probe size and material properties.

We now compute the frequency-dependent resistance to oscillatory translations. To demonstrate the impact that fluid inertia can have on probe motion, we consider a sphere that oscillates with velocity $\mathbf{V}_0 e^{i\omega t}$, such that the fluid velocity, pressure, and stress fields have the form

$$\{\mathbf{v}, p, \boldsymbol{\sigma}\} = \{\mathbf{v}_0, p_0, \boldsymbol{\sigma}_0\} e^{i\omega t} \tag{2.84}$$

The Stokes equations (2.29) for viscous flow would then take the form

$$i\omega\rho\mathbf{v}_0 = -\nabla p_0 + \eta\nabla^2\mathbf{v}_0 \tag{2.85}$$

$$\nabla \cdot \mathbf{v}_0 = 0, \tag{2.86}$$

subject to boundary conditions

$$\mathbf{v}_0|_{r=a} = \mathbf{V}_0 \tag{2.87}$$

$$\mathbf{v}_0(r \to \infty) \to \mathbf{0}. \tag{2.88}$$

The stress field $\boldsymbol{\sigma}_0$ can be computed from the pressure (p_0) and velocity ($\mathbf{v}_0$) fields,

$$\boldsymbol{\sigma}_0 = -p_0\boldsymbol{\delta} + \eta\left(\nabla\mathbf{v}_0 + (\nabla\mathbf{v}_0)^T\right), \tag{2.89}$$

so that the drag force

$$\mathbf{F}^f(t) = \mathbf{F}_0^f e^{i\omega t} \tag{2.90}$$

exerted by the fluid on the probe is given by

$$\mathbf{F}_0^f = \int_{|\mathbf{r}|=a} \hat{\mathbf{n}} \cdot \boldsymbol{\sigma}_0 dA. \tag{2.91}$$

Stokes (1850) solved this problem while studying the influence of fluid inertia on the oscillations of pendula. Schieber *et al.* (2013) detail the history and solution of this problem, and place it within the context of microrheology.

The stream function

$$\psi(r,\theta,t) = \psi_0(r,\theta,\omega)e^{i\omega t} \tag{2.92}$$

for a sphere oscillating with frequency ω is given by

$$\frac{\psi_0(r,\theta,\omega)}{V_0 \sin^2\theta} = \frac{3a}{2\Gamma^2 r}\left((1+\Gamma r)e^{-\Gamma(r-a)} - (1+\Gamma a)\right) - \frac{a^3}{2r}, \tag{2.93}$$

where

$$\Gamma(\omega) = (1+i)\sqrt{\frac{\rho\omega}{2\eta}} = \frac{1+i}{\lambda_V}, \tag{2.94}$$

and where

$$\lambda_V = \sqrt{\frac{2\eta}{\rho\omega}} \tag{2.95}$$

is the oscillatory boundary layer thickness as in eqn 2.50.

Velocity and pressure fields can be derived from eqn 2.93 using (2.68–2.69), giving

$$\frac{v_r}{V_0\cos\theta} = 3\frac{a}{r}\left(\frac{1+a\Gamma-(1+\Gamma r)e^{-\Gamma(r-a)}}{\Gamma^2 r^2}\right) + \frac{a^3}{r^3} \tag{2.96}$$

$$\frac{v_\theta}{V_0\sin\theta} = 3\frac{a}{r}\left(\frac{1+\Gamma a-(1+\Gamma r+\Gamma^2 r^2)e^{-\Gamma(r-a)}}{2\Gamma^2 r^2}\right) + \frac{a^3}{2r^3} \tag{2.97}$$

$$\frac{p}{V_0\cos\theta} = i\omega\rho a\frac{3+3\Gamma a+\Gamma^2 a^2}{2\Gamma^2 r^2}, \tag{2.98}$$

from which the force exerted by the fluid on the sphere can be computed as

$$\mathbf{F}_0^f = -6\pi\eta a\left(1+\Gamma a+\frac{\Gamma^2 a^2}{9}\right)\mathbf{V}_0, \tag{2.99}$$

or

$$\mathbf{F}_0^f = -\zeta_0\left(1+\frac{a}{\lambda_V}+i\frac{a}{\lambda_V}\right) - iM_f\omega\mathbf{V}_0. \tag{2.100}$$

Here

$$M_f = \frac{1}{2}\frac{4\pi a^3 \rho_f}{3} \tag{2.101}$$

is the so-called added mass of the fluid, which represents the equivalent mass of fluid that must be accelerated to make way for the oscillating sphere.

The inertia of the fluid thus changes the hydrodynamic resistance $\zeta^*(\omega)$,

$$\zeta^*(\omega) = 6\pi\eta a\,(1 - \Gamma(\omega)a) + iM_f\omega \tag{2.102}$$

$$\zeta^*(\omega) = 6\pi\eta a\left(1 + \frac{a}{\lambda_V} + i\frac{a}{\lambda_V}\right) + iM_f\omega \tag{2.103}$$

giving it both real and imaginary components.

Physically, λ_V corresponds to the distance vorticity (momentum) that diffuses into the fluid during one oscillation period. The resistance (eqn 2.103) shows qualitatively distinct limits, depending on the relative size of the sphere radius a compared with the oscillatory penetration depth λ_V. Since λ_V depends on ω, a natural "inertial" frequency emerges,

$$\omega_I = \frac{2\eta}{\rho a^2}, \tag{2.104}$$

which corresponds to the oscillation frequency above which inertia dominates the resistance to oscillation, and below which viscous stresses dominate the resistance. For reference, a microrheological probe of order $a \sim 1\ \mu$m in water (for which $\nu \sim 10^{-2}\text{cm}^2/\text{s}$) has an inertial frequency $\omega_I \sim 2 \times 10^6/\text{s}$.

At low frequencies ($\omega \ll \omega_I$), which corresponds to $a/\lambda_V \ll 1$, the sphere moves quasi-steadily, with a resistance

$$\zeta^*\,(\omega \ll \omega_I) \to \zeta_0\left(1 + \frac{a}{\lambda_V}\right) + i\zeta_0\frac{a}{\lambda_V}, \tag{2.105}$$

that predominantly reflects Stokes drag, with a minor correction due to inertia.

In the opposite limit of high frequencies ($\omega \gg \omega_I$), so that $a/\delta \gg 1$, the hydrodynamic resistance becomes predominantly imaginary,

$$\zeta^*(\omega) \sim \frac{4\pi\eta a^3 i}{3\lambda_V^2} = iM_f\omega. \tag{2.106}$$

Finally, the force on a sphere moving with an arbitrary (but "small") velocity history $\mathbf{V}(t)$ can be constructed by Fourier-transforming $\mathbf{V}(t)$,

$$\tilde{\mathbf{V}}(\omega) = \int_{-\infty}^{\infty} \mathbf{V}(t) e^{-i\omega t} dt, \tag{2.107}$$

then using eqn 2.99 to determine the force due to each frequency component $\tilde{V}(\omega)$, and computing the inverse transform. This gives

$$\mathbf{F}(t) = -6\pi\eta a \mathbf{V}(t) - M_f \frac{d\mathbf{V}}{dt} - 6a^2\sqrt{\pi\eta\rho} \int_{-\infty}^{t} \frac{d\mathbf{V}(\tau)}{d\tau} \frac{d\tau}{\sqrt{(t-\tau)}}. \tag{2.108}$$

The first term is the standard, quasi-steady Stokes drag; the second term represents the added mass, accouting for the inertia of the fluid that must be accelerated as the velocity changes. The third term is the Basset "memory" term (Basset, 1888), and shows the resistance depending on the sphere's previous acceleration history.

Exercise 2 concerns an analogous problem—a sphere oscillating in a purely elastic medium—for which

$$\mathbf{F}_0 = -6\pi G a (1 - a\Gamma_E)\mathbf{U}_0 + \frac{1}{2} M_f \omega^2 \mathbf{U}_0, \tag{2.109}$$

where

$$\Gamma_E = \sqrt{\frac{\rho\omega^2}{G}} = \frac{\omega}{c}, \tag{2.110}$$

or equivalently

$$\mathbf{F}_0 = -6\pi G a \left(1 - \frac{a}{c}\omega\right) \mathbf{U}_0 + \frac{1}{2} M_f \omega^2 \mathbf{U}_0. \tag{2.111}$$

The complex spring constant becomes

$$\kappa^*(\omega) = 6\pi G a (1 - a\Gamma_E) - \frac{1}{2} M_f \omega^2. \tag{2.112}$$

Exercise 2.3 asks the reader to show that the Correspondence Principle can be used to derive these results from the analogous results for viscous fluids, and vice versa. Because the spring constant and resistance are related via

$$\kappa^*(\omega) = i\omega\zeta^*(\omega), \tag{2.113}$$

eqn 2.112 can be written

$$\zeta^*(\omega) = \frac{6\pi Ga}{i\omega}\left(1 - a\Gamma_E\right) + \frac{i}{2}M_f\omega. \tag{2.114}$$

Finally, incompressible, viscoelastic materials have complex shear moduli

$$G^* = G_0 e^{i\delta} \tag{2.115}$$

where δ ranges between 0 for elastic media and $\pi/2$ for purely viscous fluids, and where both G_0 and δ depend on frequency ω. The Correspondence Principle immediately yields the relevant results for spheres oscillating in such materials, *e.g.*, by substituting

$$\Gamma_E^* = \omega\sqrt{\frac{\rho}{G^*}} = \Gamma_E e^{-i\delta/2} \tag{2.116}$$

for Γ_E in eqn 2.112, giving

$$\tilde{\kappa}^*(\omega) = 6\pi G_0 e^{i\delta} a\left(1 - a\Gamma_E e^{-i\delta/2}\right) - \frac{1}{2}M_f\omega^2, \tag{2.117}$$

or alternatively

$$\zeta^*(\omega) = \frac{6\pi G^*(\omega)a}{i\omega}\left(1 - a\Gamma_E e^{-i\delta/2}\right) + \frac{i}{2}M_f\omega. \tag{2.118}$$

2.5.4 Particle inertia

Thus far, we have neglected the inertia of the probe in treating its dynamics. In this case, the force $\mathbf{F}^p$ driving a probe into motion is exactly balanced by the drag force $\mathbf{F}^f$ exerted by the medium on the particle

$$\mathbf{F}^p + \mathbf{F}^f = \mathbf{0}. \tag{2.119}$$

Probes accelerate during unsteady motion, however, which are balanced by the inertia of the probe, giving

$$\mathbf{F}^p + \mathbf{F}^f = m_p\ddot{\mathbf{U}}_p. \tag{2.120}$$

Probes that oscillate with frequency ω obey the force balance

$$\mathbf{F}_0^p + \mathbf{F}_0^f = -M_p\omega^2\mathbf{U}_0 = i\omega M_p\mathbf{V}_0. \tag{2.121}$$

Using eqn 2.99 for the drag force from the fluid gives

$$\mathbf{F}_0^p = \zeta_0\mathbf{V}_0\left(1 + \frac{a}{\lambda_V}\right) + i\left(\frac{a}{\lambda_V}\zeta_0 + \omega(M_f + M_p)\right)\mathbf{V}_0. \tag{2.122}$$

2.5.5 Spheres forced within compressible elastic media

The elastic-displacement field around a sphere of radius a subject to a force $\mathbf{F}$ in a compressible elastic medium with shear and bulk moduli G and K is given by

$$\mathbf{u}(\mathbf{r}) = \frac{\mathbf{F}}{8\pi Gb} \cdot \left[(2b-1)\,\frac{\boldsymbol{\delta}}{r} + \frac{\mathbf{rr}}{r^3} \right] - \frac{a^2}{3}\frac{\mathbf{F}}{8\pi Gb} \cdot \left[-\frac{\boldsymbol{\delta}}{r} + 3\frac{\mathbf{rr}}{r^3} \right], \quad (2.123)$$

or, in index notation,

$$u_i(\mathbf{r}) = \frac{F_j}{8\pi Gb} \left[(2b-1)\,\frac{\delta_{ij}}{r} + \frac{r_i r_j}{r^3} \right] - \frac{a^2}{3}\frac{F_j}{8\pi Gb} \left[-\frac{\delta_{ij}}{r} + 3\frac{r_i r_j}{r^3} \right], \quad (2.124)$$

where

$$b = 2(1-\nu) = \frac{3K+4G}{3K+G}. \quad (2.125)$$

Note that $b \to 1$ in the incompressible limit ($K \gg G$).

Just like for Stokes flow (Section 2.5.2), the displacement field around a forced sphere can be decomposed into two contributions. The first is Thomson's solution (Thomson, 1848) for the field due to a point force in a compressible elastic medium,

$$\mathbf{u}(\mathbf{r}) = \frac{\mathbf{F}}{8\pi Gb} \cdot \left[(2b-1)\,\frac{\boldsymbol{\delta}}{r} + \frac{\mathbf{rr}}{r^3} \right]. \quad (2.126)$$

which is the analog of the Oseen Tensor (eqn 2.82) for compressible elastic media. For incompressible materials ($K \gg G$, for which $b = 1$), in fact, eqn 2.126 reduces exactly to the Oseen tensor (eqn 2.82) when the Correspondence Principle is used to convert between elastic and viscous solutions, as the reader is asked to show in Exercise 2.5). The second term in eqn 2.123 is a point-source dipole—irrotational and incompressible—just as in a viscous fluid.

Evaluating the displacement field at the sphere's boundary $r = a$ gives the sphere displacement $\mathbf{U}$,

$$\mathbf{U} = \mathbf{u}(a) = \frac{\mathbf{F}}{12\pi Gab}(3b-1) = \frac{\mathbf{F}}{6\pi Ga}\left(\frac{6K+11G}{6K+8G}\right). \quad (2.127)$$

Notably, from the incompressible limit $K/G \to \infty$, we recover

$$\mathbf{U}(K \gg G) \to \frac{\mathbf{F}}{6\pi Ga}, \quad (2.128)$$

as required by the Correspondence Principle.

In their F-actin microrheology studies, Schnurr *et al.* (1997) discuss the small impact that finite compressibility plays in eqn 2.127. In the limit of a highly compressible material, $K \ll G$ (or in terms of the Poisson ratio, as it approaches $\nu = -1$), the sphere displacement becomes

$$\mathbf{U}(K \ll G) \rightarrow \frac{\mathbf{F}}{6\pi G a} \cdot \frac{11}{8}, \tag{2.129}$$

which is only about 40% larger than it would move within an incompressible medium with the same shear modulus. This relatively small contribution explains, in part, why compressibility has generally been ignored in the microrheology literature. Moreover, most soft materials probed in microrheology tend to consist of an elastic meso-structure immersed in an incompressible fluid, which must "drain" through for the material to deform compressibly, as discussed by Schnurr *et al.* (1997), Gittes *et al.* (1997), and Levine and Lubensky (2001), and will be explored in Section 2.7.

For reference, we note that Oestricher (1951) computed the resistance of a sphere to oscillatory translations in compressible viscoelastic media (for which $G^*(\omega)$ and $K^*(\omega)$ are both frequency-dependent, which Norris (2006) generalized to allow for particle/medium slip. In fact, Oestricher recognized the Correspondence Principle in his study as well.

2.6 Hydrodynamic interactions

We have thus far examined the behavior of individual particles in infinite media. In practice, however, experimental sample cells are finite, with *e.g.*, glass slides and cover slips bounding the material. Hydrodynamic interactions between the probe and fluid boundaries changes the probe's response to applied forces (*i.e.*, the mobility and resistance of the probes). Since a common goal of microrheology is to use measured probe mobilities to extract rheological properties intrinsic to the material, it is important to quantify the impact of these interactions (*e.g., probe-wall hydrodynamic interactions*), so as to avoid misinterpreting nearby walls as material rheology.

Hydrodynamic interactions need not only be deleterious, but may be specifically exploited. For example, "two-point" microrheology (Section 4.11) uses correlations between two Brownian probes, which depend explicitly on their hydrodynamic interactions, to measure the rheology of the material located between them.

We will next discuss how to treat these hydrodynamic interactions, and will focus specifically on the two systems mentioned here:

Hydrodynamic interactions between two spherical probes, which forms the basis of *two-point microrheology*, and hydrodynamic interactions between a probe and a wall, which must be accounted for to correctly infer the rheology.

2.6.1 Method of reflections

Simple, closed-form solutions (like those presented for the motion of an isolated sphere) are no longer available once walls or multiple spheres are present. In typical microrheology experiments, however, probe particles are generally well-separated (from walls or from each other). This separation enables a powerful approximation technique, generally called the method of reflections (Kim and Karilla, 1991; Leal, 2007; Pozrikidis, 1992), which can produce a series expansion that accounts for hydrodynamic interactions in the resistance or mobility of probes.

The essence of the strategy is to recognize that well-separated particles behave approximately as isolated particles, and therefore establish velocity fields that are very nearly like those in infinite space. These "isolated probe" velocity fields violate the boundary conditions on other particles or walls, however. In order to "fix" this violated-boundary condition, a "reflected" velocity field is computed as though that particle (or wall) were alone in the world. This first reflected velocity field, however, violates the no-slip boundary condition on the original probe. A second reflection is thus computed to fix this violation, again for an isolated sphere, which once again violates the boundary condition on the wall or second probe, and so on. Ultimately, the method of reflections produces a power series expansion in powers of a/d, where d is the distance between the probe and the wall, or between the probe and a second particle.

The full method of reflections requires additional concepts and results from viscous hydrodynamics. In many cases, however, only the leading-order correction of hydrodynamic interactions to the probe mobility is required. We will therefore detail this first reflection here, and leave the advanced treatment to Section 2.6.5.

The key question concerns how a particle responds when the fluid around it is moving. Remember that inertia is usually negligible in the low-Re limit relevant to typical microrheology experiments. Rather than $\mathbf{F} = M\mathbf{a}$, then, the probe typically responds via $\mathbf{F} = \zeta\mathbf{V}$ (eqn 2.58). That is, a force $\mathbf{F}$ must be exerted on a probe in order for that probe to move *through* the local fluid. If no force is exerted on the probe, then the probe simply moves with the local-fluid velocity.

To the leading order, then, a probe immersed in a fluid with some velocity field $\mathbf{v}_\infty(\mathbf{r})$ at some position $\mathbf{r}_p$ moves with approximate velocity

$$V_p \sim \mathbf{v}_\infty(\mathbf{r}_p) \tag{2.130}$$

unless some force prevents it from doing so.

This simple notion now allows HI to be computed directly for the key situations we have described.

2.6.2 Hydrodynamic interactions between spheres in incompressible media

We first start by computing the hydrodynamic coupling between two well-separated spherical probes, each of radius a, located at the origin ($\mathbf{r}_1 = \mathbf{0}$) and $\mathbf{r}_2 = d\hat{\mathbf{r}}$, respectively (Fig. 2.9).[6] We will assume that the distance of separation d between the probes is much larger than the probe radii, so that $a/d \ll 1$. This is the key computation required for two-point microrheology (Section 4.11).

If a force $\mathbf{F}_1$ is exerted on particle 1, what is the velocity $\mathbf{V}_2$ of particle 2 in response? This relation is called the *coupling mobility* b_{21} between the spheres, and will be computed here.

The force on probe 1 drives it into motion with velocity given approximately by

$$\mathbf{V}_1 \approx \frac{\mathbf{F}_1}{6\pi\eta a}, \tag{2.131}$$

and establishes a velocity field $\mathbf{v}_1(\mathbf{r})$ that can be well-approximated as that around an isolated sphere in an infinite fluid eqn 2.70,

$$\mathbf{v}_1(\mathbf{r}) = \frac{1}{8\pi\eta r}\left(\mathbf{F}_1 + (\mathbf{F}_1\cdot\hat{\mathbf{r}})\hat{\mathbf{r}}\right) + \frac{a^2}{24\pi\eta r^3}\left(\mathbf{F}_1 - 3(\mathbf{F}_1\cdot\hat{\mathbf{r}})\hat{\mathbf{r}}\right). \tag{2.132}$$

How does the second particle respond to the forced motion of the first particle? Strictly speaking, the second particle does not "know" that the first particle even exists, nor that it is moving. Rather, the second particle is immersed in a fluid that has been set into motion by the force on the first. If no force is exerted on particle 2, then it simply moves with the local velocity of the fluid in its immediate vicinity,

$$\mathbf{V}_2 \approx \mathbf{v}_1(\mathbf{r}_2). \tag{2.133}$$

Since we are only treating the leading-order correction due to hydrodynamic interactions, we must keep only the leading-order term in

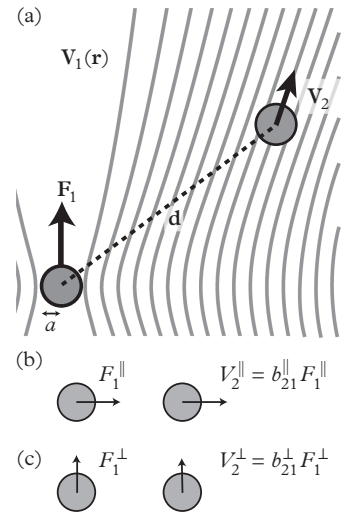

Fig. 2.9 ***Hydrodynamic interactions between spheres*** *(a) Two well-separated spheres, each of radius a, are separated by a distance d in a viscous fluid, where $d \gg a$. A force $\boldsymbol{F}_1$ on sphere 1 drives the surrounding fluid to flow with velocity field $\boldsymbol{v}_1(\boldsymbol{r})$, which causes sphere 2 to move with velocity $\boldsymbol{V}_2 = \boldsymbol{b}_{21}\cdot\boldsymbol{F}_1$, where $\boldsymbol{b}_{21}$ is the coupling mobility tensor. Analysis is simplified by decomposing this system into force-components parallel (b) and perpendicular (c) to the separation vector $\boldsymbol{d}$. Sphere 2 moves with velocities $\boldsymbol{V}_2^{\parallel}$ and $\boldsymbol{V}_2^{\perp}$ in response to parallel and perpendicular force components $\boldsymbol{F}_1^{\parallel}$ and $\boldsymbol{F}_1^{\perp}$ on sphere one, which defines the parallel and perpendicular coupling mobilities $b_{21}^{\parallel}$ and $b_{21}^{\perp}$, respectively. Both are functions of the relative-separation d/a, and given by eqns 2.136–2.137.*

[6] Exercise 8 treats the problem with different-sized spheres.

the far-field velocity field driven by sphere 1,[7] which is the Stokeslet term

$$\mathbf{v}_1(\mathbf{r}_2) \approx \mathbf{G}^{\mathrm{St}}(\mathbf{r}_2) \cdot \mathbf{F}_1. \tag{2.134}$$

A freely-suspended particle 2 thus responds to a force $\mathbf{F}_1$ on particle 1 by moving with approximate velocity

$$\mathbf{V}_2 = \frac{\hat{\mathbf{x}} \cdot \mathbf{F}_1}{4\pi\eta d}\hat{\mathbf{x}} + \frac{\hat{\mathbf{y}} \cdot \mathbf{F}_1}{8\pi\eta d}\hat{\mathbf{y}} + \frac{\hat{\mathbf{z}} \cdot \mathbf{F}_1}{8\pi\eta d}\hat{\mathbf{z}}. \tag{2.135}$$

Several features in eqn 2.135 are noteworthy. First, the leading-order approximation to the coupling mobility does not depend on the size of either probe! In fact, it does not even depend on the shape of either probe, so long as the separation distance d between particles significantly exceeds the longest dimension of either particle. This reflects two key facts. The first is that the far-field flow around the forced particle is dominated by the Stokeslet—which depends only on the force that is exerted, rather than the shape or size of the particle to which it is exerted. Second, particle 2 is not forced through the fluid, but rather simply moves along with whatever velocity the fluid is moving. That is—particle 2 does not move because it is forced to; it moves because it is *not* forced *not* to move, and simply moves with whatever velocity its surroundings move. Neither the forced flow, nor the advection velocity, cares about the size or shape of either probe, to the leading order.

Second, the velocity (eqn 2.135) is anisotropic: Particle 2 moves twice as fast when the force $\mathbf{F}_1$ is directed *toward* particle 2 (*i.e.*, $\mathbf{F}_1 = F\hat{\mathbf{x}}$),

$$V_2^{\parallel} = \frac{1}{4\pi\eta d}F_1^{\parallel} \equiv b_{21}^{\parallel}F_1^{\parallel} \tag{2.136}$$

than when the force $\mathbf{F}_2$ is directed *perpendicular* to the vector separating the particle pair,

$$V_2^{\perp} = \frac{1}{8\pi\eta d}F_1^{\perp} \equiv b_{21}^{\perp}F_1^{\perp}. \tag{2.137}$$

The coupling mobility is therefore an *anisotropic* tensor,

$$\mathbf{b}_{21} = \mathbf{G}^{\mathrm{St}}(\mathbf{r}_2). \tag{2.138}$$

Likewise, a force $\mathbf{F}_2$ on particle two drives it to move with velocity

$$\mathbf{V}_2 \approx \frac{\mathbf{F}_2}{6\pi\eta a} \tag{2.139}$$

[7] The faster decay of the source doublet flow in 2.132 makes its contribution smaller than the leading-order (Stokeslet) contribution by an amount of order $(a/d)^2$. Correctly computing this correction requires the curvature of $\mathbf{v}_1(\mathbf{r})$ to be treated properly, using Faxen's law, and is described in Section 2.6.5.

and drives particle 1 to move with velocity

$$\mathbf{V}_1 = \frac{\hat{\mathbf{x}}\cdot\mathbf{F}_2}{4\pi\eta d}\hat{\mathbf{x}} + \frac{\hat{\mathbf{y}}\cdot\mathbf{F}_2}{8\pi\eta d}\hat{\mathbf{y}} + \frac{\hat{\mathbf{z}}\cdot\mathbf{F}_2}{8\pi\eta d}\hat{\mathbf{z}}. \tag{2.140}$$

One can thus construct a multiparticle mobility tensor,

$$\begin{pmatrix}\mathbf{V}_1\\ \mathbf{V}_2\end{pmatrix} = \begin{pmatrix}\mathbf{b}_{11} & \mathbf{b}_{12}\\ \mathbf{b}_{21} & \mathbf{b}_{22}\end{pmatrix}\cdot\begin{pmatrix}\mathbf{F}_1\\ \mathbf{F}_2\end{pmatrix}, \tag{2.141}$$

where each $\mathbf{b}_{ij}$ represents a 3×3 mobility tensor, diagonal blocks representing self-mobilities,

$$\mathbf{b}_{ii} = \frac{1}{6\pi\eta a}\boldsymbol{\delta}, \tag{2.142}$$

and off-diagonal blocks represent coupling mobilities by the Oseen tensor:

$$\mathbf{b}_{i\neq j} = \frac{1}{8\pi\eta d}\left(\boldsymbol{\delta} + \hat{\mathbf{d}}\hat{\mathbf{d}}\right), \tag{2.143}$$

where

$$\hat{\mathbf{d}} = \frac{\mathbf{r}_2 - \mathbf{r}_1}{|\mathbf{r}_2 - \mathbf{r}_1|}. \tag{2.144}$$

To illustrate, consider forces $\mathbf{F}_1$ and $\mathbf{F}_2$ directed parallel to $\hat{\mathbf{d}}$ (the line between the particles), as in Fig. 2.10. In this case, the two-particle mobility tensor, valid to $\mathcal{O}\left(\frac{a}{d}\right)$, is given by

$$\begin{pmatrix}V_1^{\parallel}\\ V_2^{\parallel}\end{pmatrix} = \frac{1}{6\pi\eta a}\begin{pmatrix}1 & \frac{3}{2}\frac{a}{d}\\ \frac{3}{2}\frac{a}{d} & 1\end{pmatrix}\cdot\begin{pmatrix}F_1^{\parallel}\\ F_2^{\parallel}\end{pmatrix}. \tag{2.145}$$

Diagonalizing shows how hydrodynamic interactions affect multiparticle dynamics, as two distinct eigenmodes appear.

$$\begin{pmatrix}V_C^{\parallel}\\ V_R^{\parallel}\end{pmatrix} = \frac{1}{6\pi\eta a}\begin{pmatrix}1+\frac{3}{2}\frac{a}{d} & 0\\ 0 & 1-\frac{3}{2}\frac{a}{d}\end{pmatrix}\cdot\begin{pmatrix}F_C^{\parallel}\\ F_R^{\parallel}\end{pmatrix} \tag{2.146}$$

One mode (denoted C) is "collective", in which forces on particles point in the same direction, so that hydrodynamic interactions contribute to each sphere's own force-driven velocity. By contrast, forces on the particles in the relative mode (denoted R) are oppositely-directed, so that hydrodynamic interactions act against the velocity

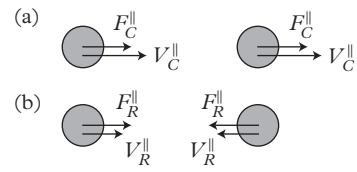

Fig. 2.10 ***Collective and Relative motion of two spheres with hydrodynamic interactions.*** *Hydrodynamic interactions give rise to two eigenmodes: (a) Collective mode, where the force on each sphere is equal in magnitude and direction, and (b) Relative mode, where forces are equal in magnitude, but oppositely directed. In the collective mode, hydrodynamic interactions impart particle velocities in the direction each was forced, giving an eigenmobility* $b_C^{\parallel} = b_0(1 + 3a/2d)$ *that is higher than the isolated-particle mobility. In the relative mode, hydrodynamic interactions contribute a velocity directed against the velocity each particle is forced to move, giving a lower eigenmobility* $b_R^{\parallel} = b_0(1 - 3a/2d)$.

with which each sphere would move if in isolation. The two eigenmobilities,

$$b_C^{\parallel} = b_0(1 + 3a/2d) \tag{2.147}$$

$$b_R^{\parallel} = b_0(1 - 3a/2d), \tag{2.148}$$

are thus enhanced and reduced for collective and relative modes, respectively.

The analogous calculation for particles forced *perpendicular* to $\hat{\mathbf{d}}$ gives weaker hydrodynamic interactions:

$$b_{R,C}^{\perp} = b_0(1 \mp 3a/4d), \tag{2.149}$$

as shown in Exercise 2.9.

2.6.3 Hydrodynamic interactions in compressible media

Compressibility affects the hydrodynamic interactions between suspended particles. As in Fig. 2.9, we consider two probes separated by a distance d, and compute the displacement $\mathbf{U}_2$ of probe 2 in response to a force $\mathbf{F}_1$ on sphere 1. It is most convenient to decompose the applied force into components that are parallel $F_1^{\parallel}$ and perpendicular $F_1^{\perp}$ to the line between the two particles (Fig. 2.10).

From the displacement field around a spherical probe eqn 2.123, we identify the slowest-decaying component as that due to the point force (Thomson's solution, eqn 2.126). As described in Section 2.6.2, a particle immersed in a medium will simply move along with its local-material environment (to leading order), unless some force is exerted on it to make it act otherwise. We must therefore simply evaluate the point-force displacement field eqn 2.126 at the center $\mathbf{r}_2$ of the second probe, to determine the leading-order approximation for the velocity of probe 2 in response to a force on probe 1. The parallel and perpendicular velocities are

$$U_2^{\parallel} = \frac{F^{\parallel}}{8\pi G d}\left(\frac{3K + 7G}{3K + 4G}\right) \tag{2.150}$$

$$U_2^{\perp} = \frac{F^{\perp}}{4\pi G d}. \tag{2.151}$$

Notably, the velocity *perpendicular* to the line of centers does not depend on material compressibility. The velocity *parallel* to the line

of centers, on the other hand, depends on both moduli. In the incompressibility limit $K/G \to \infty$, these results are consistent with incompressible Stokes flows, as the Correspondence Principle would suggest. Because the parallel and perpendicular resistances depend on K and G in distinct ways, independent measurements of these two quantities would enable the two moduli to be extracted. This statement can also be read in reverse: Because this material has two distinct material parameters, two "linearly independent" measurements are required to properly characterize the material.

Lastly, note that the coupling mobility decays with separation like d^{-1}, whether or not the material has finite compressibility. As with incompressibility, the coupling mobility does not depend on the size or shape of either probe, so long as they are well-separated.

2.6.4 Particle-wall hydrodynamic interactions: Confinement effects

In practice, all experimental systems are finite in extent, and are typically bounded by either solid walls. Walls interact hydrodynamically with particles, which changes the probe mobility in a way that could be misinterpreted as rheology. It is therefore important to understand the magnitude of confinement effects inherent to practical sample cells, and their impact on the interpretation of microrheology experiments.

To do so, we follow a similar strategy as we did for interparticle-hydrodynamic interactions. A forced particle sets up a flow that is approximately that of an isolated sphere. This flow, however, violates the no-slip condition on a rigid wall. We then must compute a new fluid velocity field that "corrects" this error on the boundary conditions at the wall. The probe forced particle thus "sees" its environment moving at the velocity set up by the wall, and simply moves along with its world.

We first consider a sphere of radius a, located a distance $z = h$ from a solid wall located at $z = 0$ (Fig. 2.11). The no-slip condition is imposed on the solid wall. A force $\mathbf{F}$ exerted on an isolated probe would set up a velocity field

$$\mathbf{v}(\mathbf{r}) = \frac{1}{8\pi\eta R_p}\left[\left(\mathbf{F} + (\mathbf{F}\cdot\hat{\mathbf{R}}_p)\hat{\mathbf{R}}_p\right) + \frac{a^2}{3R_p^2}\left(\mathbf{F} - 3(\mathbf{F}\cdot\hat{\mathbf{R}}_p)\hat{\mathbf{R}}_p\right)\right], \tag{2.152}$$

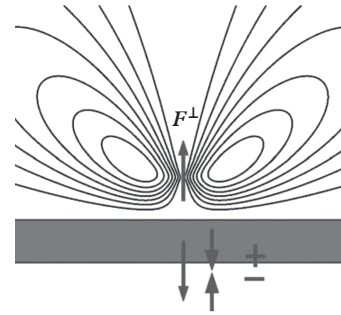

Fig. 2.11 ***Probe-wall hydrodynamic interactions.*** *(a) The flow field due to a point force located a distance h from a no-slip surface consists of (b) the Stokeslet flow due to the point force at $h\hat{\mathbf{z}}$, and (c) a wall flow $\boldsymbol{v}_w$ established by a Stokeslet, Stokeslet doublet, and Source Dipole located at the "image" location $\boldsymbol{r}_i = -h\hat{\mathbf{z}}$. (d) The velocity of a forced sphere near a wall is given approximately by the self-mobility $b_0\boldsymbol{F}_1$ due to the force (b), with a correction $\boldsymbol{v}_w(\boldsymbol{r}_p - \boldsymbol{r}_i)$ given by the velocity with which the wall flow advects the sphere, given by eqns 2.161–2.162.*

where $\mathbf{R}_p$ is the vector between the observation point (at $\mathbf{r}$) and the probe (at $h\hat{\mathbf{z}}$):

$$R_p = \sqrt{x^2 + y^2 + (z-h)^2} \tag{2.153}$$

$$\hat{\mathbf{R}}_p = \frac{\mathbf{r} - h\hat{\mathbf{z}}}{R_p}. \tag{2.154}$$

As mentioned earlier, this force would drive the probe to move with velocity

$$\mathbf{V} = (6\pi\eta a)^{-1}\mathbf{F} \tag{2.155}$$

if it were isolated.

We here assume the sphere is located far from the wall, meaning that $h \gg a$. Far from the particle ($R_p \gg a$), the fluid velocity field (2.152) is given approximately by the Stokeslet (point force) flow,

$$\mathbf{v}(\mathbf{r}) = \frac{1}{8\pi\eta R_p}\left(\mathbf{F} + (\mathbf{F}\cdot\hat{\mathbf{R}}_p)\hat{\mathbf{R}}_p\right) \equiv \mathbf{F}\cdot\mathbf{G}^{\mathrm{St}}(\mathbf{R}_p) \tag{2.156}$$

which does not vanish on the wall (at $z = 0$), in violation of the no-slip boundary condition.

Blake (1971) showed that a simple set of image singularities, located behind the wall at $z = -h$, fixes the no-slip boundary condition on the wall (Fig. 2.11). The image flow field to correct the no-slip condition for a point force $\mathbf{F}_\perp = F_\perp\hat{\mathbf{z}}$ *perpendicular* to a nearby wall is given by

$$\mathbf{v}_w^\perp(\mathbf{r}) = \left[-\mathbf{G}^{\mathrm{St}}(\mathbf{R}_i) + 2h^2\mathbf{G}^{\mathrm{PD}}(\mathbf{R}_i) - 2h\mathbf{G}^{\mathrm{StD}}(\mathbf{R}_i)\right]\cdot\mathbf{F}_\perp, \tag{2.157}$$

where

$$\mathbf{R}_i = \mathbf{r} + h\hat{\mathbf{z}} \tag{2.158}$$

is the vector from the image position ($-h\hat{\mathbf{z}}$) and the observation point $\mathbf{r}$, $\mathbf{G}^{\mathrm{PD}}(\mathbf{R}_i)$ represents the flow at $\mathbf{r}$ due to a potential dipole (eqn 2.83) located at $-h\hat{\mathbf{z}}$, and $\mathbf{G}^{\mathrm{StD}}$ is the flow due to a Stokeslet doublet, defined by

$$\mathbf{G}^{\mathrm{StD}}(\mathbf{r}) = \frac{\partial}{\partial z_0}\mathbf{G}^{\mathrm{St}}(\mathbf{r} - \mathbf{r}_0). \tag{2.159}$$

The image flow field $\mathbf{v}_w^\perp$, given by eqn 2.157, represents the flow set up by the wall in response the action of the forced probe. This image

flow field thus causes the fluid environment around the probe to move, and advects the probe. Evaluating $\mathbf{v}_w^{\perp}(\mathbf{r} = h\hat{\mathbf{z}})$ at the probe location $\mathbf{r} = h\hat{\mathbf{z}}$ gives the correction to the probe velocity due to hydrodynamic interactions with the wall,

$$\mathbf{v}_w^{\perp}(\mathbf{r} = h\hat{\mathbf{z}}) = -\frac{3F_{\perp}}{16\pi\eta}. \tag{2.160}$$

The probe mobility, perpendicular to a wall, is thus given by

$$V_{\perp} = b_0 \left(1 - \frac{9a}{8h}\right) F_{\perp}. \tag{2.161}$$

Using the image system for a Stokeslet force $\mathbf{F}_{\parallel}$ oriented parallel to the wall, the mobility of a sphere forced parallel to a wall can be shown to be

$$V_{\parallel} = b_0 \left(1 - \frac{9a}{16h}\right) F_{\parallel}. \tag{2.162}$$

In similar fashion, hydrodynamic interactions between a probe and other surfaces may be computed using the method of reflections, including liquid/gas interfaces (where a no-shear stress condition is imposed), for which the perpendicular mobility is reduced, but parallel mobility is enhanced; planar interfaces between two viscous interfaces, and partial-slip boundaries.

Key points to remember from this section are: (i) Hydrodynamic interactions with solid walls *reduce* probe mobility; (ii) the probe radius a is the "unit" distance over which hydrodynamic interactions decay, and (iii) hydrodynamic interactions are fairly long-ranged, decaying like (a/h).

2.6.5 Higher-order corrections: Faxen's law, and multiple reflections

Equations 2.143 and 2.161–2.162 give the *leading-order* approximations to the hydrodynamic interactions between two spheres and between a sphere and a well, respectively. This level of approximation will suffice for almost all results relevant to microrheology. More accurate expressions can be obtained using the *method of reflections*. We include this section primarily for those readers interested in taking the next step; more extensive discussions can be found in advanced texts in fluid mechanics and suspension mechanics—*e.g.*, Kim and Karilla (1991), Leal (2007), and Pozrikidis (1992).

We will illustrate this explicitly for the coupling mobility between spheres. Notably, eqn 2.143 only depends on the slowest-decaying (Stokeslet) component of the velocity field around the forced sphere. Including the source dipole field eqn 2.83 in the calculation is simple enough, and gives a correction that is smaller than the Stokeslet contribution by an amount of $\mathcal{O}(a^2/d^2)$.

When considering corrections this small, however, one must also account for the fact the Stokeslet velocity field (which we had evaluated at $\mathbf{r}_2$, the center of particle 2) is itself heterogeneous. To do so, we turn to Faxen's laws, which give the force $\mathbf{F}$ and torque $\mathbf{L}$ required to make a sphere of radius a, located at $\mathbf{r}_p$, translate at velocity $\mathbf{V}_p$, and rotate at angular velocity $\mathbf{\Omega}_p$ while immersed in a background flow $v_\infty(\mathbf{r})$. Specifically, Faxen's laws reveal

$$\mathbf{F} = 6\pi\eta a\left(\mathbf{V}_p - \mathbf{v}_\infty(\mathbf{r}_p) - \frac{a^2}{6}(\nabla^2\mathbf{v}_\infty)\,|_{\mathbf{r}=\mathbf{r}_p}\right) \tag{2.163}$$

$$\mathbf{L} = 8\pi\eta a^3\left(\mathbf{\Omega}_p - \frac{1}{2}\nabla\times\mathbf{v}_\infty\,|_{\mathbf{r}=\mathbf{r}_p}\right). \tag{2.164}$$

The coupling mobility of interest here relates the velocity $\mathbf{V}_2$ of sphere 2, which is force- and torque-free, in response to a force $\mathbf{F}_1$ on sphere 1. The force $\mathbf{F}_1$ on sphere 1 establishes a flow which advects sphere 2, so that the velocity field $\mathbf{v}_\infty(\mathbf{r}) = \mathbf{v}_1(\mathbf{r})$ in Faxen's laws (2.163–2.164). Because there is no force ($\mathbf{F}_2 = 0$) or torque ($\mathbf{L}_2 = 0$) on particle 2, Faxen's laws (2.163–2.164) can be re-arranged with $\mathbf{F} = \mathbf{L} = 0$ to reveal to obtain the advection velocity of particle 2,

$$\mathbf{V}_2 = \mathbf{v}_1(\mathbf{r}_2) + \frac{a^2}{6}\nabla^2\mathbf{v}_1\,|_{\mathbf{r}=\mathbf{r}_2} \tag{2.165}$$

$$\mathbf{\Omega}_2 = \frac{1}{2}\nabla\times\mathbf{v}_1\,|_{\mathbf{r}=\mathbf{r}_2}. \tag{2.166}$$

Evaluating the full (isolated) velocity field $\mathbf{v}_1$ at $\mathbf{r}_2 = d\hat{\mathbf{x}}$ gives

$$\mathbf{v}_1(d\hat{\mathbf{x}}) = \frac{1}{6\pi\eta a}\left[\left(\frac{3a}{2d} - \frac{a^3}{2d^3}\right)\mathbf{F}_1^{\parallel} + \left(\frac{3a}{4d} + \frac{a^3}{4d^3}\right)\mathbf{F}_1^{\perp}\right] \tag{2.167}$$

and

$$\frac{a^2}{6}\nabla^2\mathbf{v}_1\,|_{d\hat{\mathbf{x}}} = \frac{1}{6\pi\eta a}\left[-\frac{a^3}{2d^3}\mathbf{F}_1^{\parallel} + \frac{a^3}{4d^3}\mathbf{F}_1^{\perp}\right] \tag{2.168}$$

so that

$$\mathbf{V}_2 = \frac{1}{6\pi\eta a}\left[\left(\frac{3a}{2d} - \frac{a^3}{d^3}\right)\mathbf{F}_1^{\parallel} + \left(\frac{3a}{4d} + \frac{a^3}{2d^3}\right)\mathbf{F}_1^{\perp}\right]. \tag{2.169}$$

The parallel and perpendicular coupling mobilities are thus

$$b_{\parallel} = \frac{1}{4\pi\eta d}\left(1 - \frac{2a^2}{3d^2}\right) \tag{2.170}$$

$$b_{\perp} = \frac{1}{8\pi\eta d}\left(1 + \frac{2a^2}{3d^2}\right), \tag{2.171}$$

valid to $\mathcal{O}(a^2/d^2)$.

Hydrodynamic interactions may also lead to relative rotations between spheres: A force $\mathbf{F}_1$ causes particle 2 to rotate via

$$\mathbf{\Omega}_2 = -\frac{1}{8\pi\eta d^2}\hat{\mathbf{F}}_1 \times \hat{\mathbf{d}}. \tag{2.172}$$

This basic strategy holds more generally: To compute hydrodynamic interactions, one must first compute the flow field established by the forced sphere, accurate to whatever order in a is required. In the particle-wall case, for example, this would require computing the higher-order ($\sim a^2$) correction to the flow field established by the wall, which would require the image system for a potential dipole. One must then use this flow field in Faxen's law eqn 2.165 to compute the advection velocity of the sphere.

2.7 Elastic networks in viscous liquids: The two-fluid model

Soft materials often consist of a compressible elastic microstructure immersed in an incompressible viscous liquid. Polymer gels, swollen by a good solvent, provide an illustrative example: The polymer network itself is elastic and compressible, yet the surrounding solvent is not. Consequently, regions of the elastic network may only be compressed (or dilated) if the solvent flows out of (or into) those regions, respectively. Viscous forces resist this flow, and set a time scale for the fluid to drain from the elastic network.

In the microrheology context, any probe motion that excites compressional deformations to the elastic microstructure, then, can cause problems. At sufficiently long times (or low frequencies) for the viscous liquid to drain freely from the elastic microstructure, the elastic structure does indeed compress (and dilate) around the probe, whereas the liquid simply redistributes to maintain its own incompressibility (Schnurr *et al.*, 1997; Gittes *et al.*, 1997; Levine and Lubensky, 2001). The material around the probe thus *becomes* inhomogeneous—invalidating the Correspondence Principle.

Swollen polymer gels are often described using the two-fluid model (Milner, 1993), where a displacement field $\mathbf{u}$ describes the (compressible) deformation of the elastic network, with bulk and shear moduli K and G, respectively (eqn 2.15), and a velocity field $\mathbf{v}$ describes the flow of the solvent. The momentum equation for each obeys the respective Cauchy stress equation 2.3, wherein a body force is included to account for the force that each phase exerts on the other. If the velocities of the two phases are equal everywhere, there is no body force; if, however, the fluid moves relative to the elastic network, then the fluid exerts a force on the network,

$$\mathbf{f}_b = \Gamma_\xi (\mathbf{v} - \dot{\mathbf{u}}), \tag{2.173}$$

which is equal and opposite to the force that the network exerts on the fluid. The parameter Γ_ξ describes the solvent/network coupling, which for a polymer network can be approximated by

$$\Gamma_\xi \sim \frac{\eta}{\xi^2}, \tag{2.174}$$

where ξ is a characteristic mesh spacing for the network. This form for Γ_ξ follows from treating the network as a porous medium, through which the fluid must flow (akin to Darcy flow).

The two-fluid model for a homogeneous, polymer gel is then given by

$$\rho_e \frac{\partial \dot{\mathbf{u}}}{\partial t} = \left(K + \frac{1}{3}G\right) \nabla(\nabla \cdot \mathbf{u}) + G\nabla^2 \mathbf{u} + \Gamma_\xi \left(\mathbf{v} - \frac{\partial \mathbf{u}}{\partial t}\right) \tag{2.175}$$

$$\rho_f \frac{\partial \mathbf{v}}{\partial t} = -\nabla p + \eta \nabla^2 \mathbf{v} - \Gamma_\xi \left(\mathbf{v} - \frac{\partial \mathbf{u}}{\partial t}\right), \tag{2.176}$$

where ρ_e and ρ_f represent the mass densities of the elastic and fluid phases, respectively. As we will see, finite compressibility impacts probe dynamics at low frequencies, and so we will neglect the transient-inertial terms. We will consider oscillations at frequency ω, for which the two-fluid equations become

$$0 = \left(K + \frac{1}{3}G\right) \nabla(\nabla \cdot \mathbf{u}_0) + G\nabla^2 \mathbf{u}_0 + \Gamma_\xi \left(\mathbf{v}_0 - i\omega \mathbf{u}_0\right) \tag{2.177}$$

$$0 = -\nabla p_0 + \eta \nabla^2 \mathbf{v}_0 - \Gamma_\xi \left(\mathbf{v}_0 - i\omega \mathbf{u}_0\right). \tag{2.178}$$

Compressional deformations may be isolated by taking the divergence of both equations, accounting for the incompressibility ($\nabla \cdot \mathbf{v}_0 = 0$) of the liquid,

$$0 = \left(K + \frac{1}{3}G\right) \nabla^2(\nabla \cdot \mathbf{u}_0) - i\omega \Gamma_\xi \nabla \cdot \mathbf{u}_0 \tag{2.179}$$

$$0 = -\nabla^2 p_0 + i\omega \Gamma_\xi \nabla \cdot \mathbf{u}_0. \tag{2.180}$$

The second equation reveals how compression impacts the dynamic pressure p in the fluid, whereas the first governs the dyanamics of compressive deformations. Scaling gradients with a probe radius a to treat the displacement field around a spherical probe gives

$$i\omega\Gamma_\xi(\nabla\cdot\mathbf{u}_0) = \frac{\left(K+\frac{1}{3}G\right)}{a^2}\tilde{\nabla}^2(\nabla\cdot\mathbf{u}_0), \tag{2.181}$$

revealing a natural "free-draining" frequency

$$\omega_c \sim \frac{\left(K+\frac{1}{3}G\right)}{\Gamma_\xi a^2} \sim \frac{\xi^2}{a^2}\frac{\left(K+\frac{1}{3}G\right)}{\eta} \sim \frac{\xi^2}{a^2}\frac{G}{\eta}\frac{1}{1-2\nu}. \tag{2.182}$$

At low frequencies ($\omega \ll \omega_c$), the fluid drains freely from the network, effectively decoupling from the dynamics. In this limit, the probe moves quasi-statically within a compressible medium, as described in 2.5.5. At high frequencies ($\omega \gg \omega_c$), the fluid does not have time to drain through the gel, and instead forces the network to deform as an effectively incompressible medium. For frequencies sufficiently above ω_c, both fields behave as incompressible, isotropic media, and therefore the correspondence principle holds. For low frequencies, on the other hand, the two "fluids" decouple, with different compressibilities, and so the Correspondence Principle breaks down. Notably, however, the displacement of a probe in a highly-compressible medium, with the $K \gg G$ limit given by eqn 2.129, differs from the displacement in an incompressible medium by only 40%. In this case, even thought the CP fails, it still makes reasonable predictions.

2.8 Non-isotropic probes

Axisymmetric probes. The isotropic shape of a sphere gives rise to its isotropic mobility and resistance. By contrast, the response of more generally-shaped particles depends on which direction they move in, and is described using mobility and resistance *tensors*. For example, the resistance of long, slender rods with velocity *perpendicular* to the rod axis is *twice* that for velocity *parallel* to the axis,[8]

$$\zeta^{\perp}_{\text{rod}} = 2\zeta^{\parallel}_{\text{rod}}. \tag{2.183}$$

The resistance and mobility tensors of a rod, whose axis is directed along $\hat{\mathbf{z}}$, is given by

$$\mathbf{b} = b_\parallel\begin{pmatrix}1/2 & 0 & 0\\ 0 & 1/2 & 0\\ 0 & 0 & 1\end{pmatrix}, \quad \boldsymbol{\xi} = \zeta_\parallel\begin{pmatrix}2 & 0 & 0\\ 0 & 2 & 0\\ 0 & 0 & 1\end{pmatrix}, \tag{2.184}$$

[8] Without this anisotropic mobility, flagella could not be used to propel microorganisms, or cilia to drive fluid flows!

where $\zeta_{\|} = 1/b_{\|}$. The anisotropy in *rotational* mobility and resistance is much stronger.

Translation-rotation coupling. Rotationally symmetric particles with fore-aft *asymmetry* (*e.g.*, egg-shaped particles, or asymmetric dumbells) will generally rotate when forced in any direction other than along its symmetry axis. Alternately, a screw-like body (rod-like, with chiral asymmetries) will rotate about the primary rod axis, in response to a force directed along the rod axis. Such translation-rotation coupling as

$$\mathbf{L} = \boldsymbol{\xi}_{\mathrm{RT}} \cdot \mathbf{V}, \tag{2.185}$$

appears as an off-diagonal block in a more general-resistance tensor:

$$\begin{pmatrix} \mathbf{F} \\ \mathbf{L} \end{pmatrix} = \begin{pmatrix} \boldsymbol{\xi}_T & \boldsymbol{\xi}_{TR} \\ \boldsymbol{\xi}_{RT} & \boldsymbol{\xi}_R \end{pmatrix} \cdot \begin{pmatrix} \mathbf{V} \\ \boldsymbol{\Omega} \end{pmatrix}, \tag{2.186}$$

so that $\boldsymbol{\xi}_{\mathrm{TR}}$ and $\boldsymbol{\xi}_{\mathrm{RT}}$ are 3x3 tensors that give the (drag) *force* on the particle when it rotates with angular velocity $\boldsymbol{\Omega}$, and the drag torque $\mathbf{L}$ on the particle when it translates with velocity $\mathbf{V}$. Moreover, it can be shown that the entire tensor is symmetric, implying[9]

$$\boldsymbol{\xi}_T = (\boldsymbol{\xi}_T)^T \tag{2.187}$$

$$\boldsymbol{\xi}_{\mathrm{TR}} = (\boldsymbol{\xi}_{\mathrm{RT}})^T \tag{2.188}$$

$$\boldsymbol{\xi}_R = (\boldsymbol{\xi}_R)^T. \tag{2.189}$$

The mobility tensor is given by the inverse of the resistance tensor:

$$\mathbf{b} = \begin{pmatrix} \mathbf{b}_T & \mathbf{b}_{TR} \\ \mathbf{b}_{RT} & \mathbf{b}_R \end{pmatrix} = \begin{pmatrix} \boldsymbol{\xi}_T & \boldsymbol{\xi}_{TR} \\ \boldsymbol{\xi}_{RT} & \boldsymbol{\xi}_R \end{pmatrix}^{-1}. \tag{2.190}$$

It is important to note that (2.190) does *not* imply that each component of the resistance tensor is given by the reciprocal of the equivalent component of the mobiity tensor. A generally-shaped particle that translates *without rotating* in the $\hat{z}$-direction experiences a drag force and torque given by $\boldsymbol{\xi} \cdot \hat{\mathbf{z}}$, of which the $\hat{z}$-component is ζ_{zz}. By contrast, if the same particle is allowed to settle under a force $\hat{\mathbf{z}}$, it does so with translational and rotational velocities given by $\mathbf{b} \cdot \hat{\mathbf{z}}$, of which b_{zz} gives the $\hat{z}$ component of the velocity. Physically, the two situations are distinct.

[9] More detailed descriptions can be found in Kim and Karilla (1991), Leal (2007), Happel and Brenner (1983), and Guazzelli and Morris (2012).

EXERCISES

(2.1) **Rotational mobility of a sphere**. Show that the flow field around a sphere of radius a, rotating in a viscous fluid with angular velocity $\mathbf{\Omega}$ about the $\theta = 0$ axis is

$$\mathbf{v}_\phi = \mathbf{\Omega} a \sin\theta \left(\frac{a^3}{r^3}\right). \tag{2.191}$$

Now, relate the torque $\mathbf{L}$ on the same sphere to its rotational velocity $\mathbf{\Omega}$

$$\mathbf{L} = \zeta_R \mathbf{\Omega} \text{ and } \mathbf{\Omega} = b_R \mathbf{L}, \tag{2.192}$$

to derive the rotational resistance (or mobility) of the sphere,

$$\zeta_R^{\text{sphere}} = 8\pi\eta a^3 = (b_R^{\text{sphere}})^{-1}. \tag{2.193}$$

Compare the decay of the flow field around a rotating sphere to that of a translating sphere. Compare how resistance (or mobility) depend on probe size a for translation vs. rotation.

(2.2) **Displacement field around an oscillating sphere.** Consider a sphere of radius a oscillating with displacement $\mathbf{U}_0 e^{i\omega t}$ in an isotropic, incompressible elastic medium with shear modulus G. Using the elastic analog of the stream function, show that the elastic displacement field obeys $E^4\psi + \Gamma_E^2 E^2 \psi = 0$, where $\Gamma_E = \omega\sqrt{\rho_m/G} = \omega/c$ is the frequency divided by the shear wave speed in the medium. Show the solution to be

$$\frac{\psi_0(r,\theta,\omega)}{U_0 \sin^2\theta} = -\frac{a^3}{2r} + \frac{3a}{2\Gamma_E^2 r}\left((1+\Gamma_E r)e^{-\Gamma_E(r-a)} - (1+\Gamma_E a)\right), \tag{2.194}$$

keeing only outgoing waves ($e^{i(\omega t - \Gamma_E r)}$). Derive the displacement and pressure fields, the stress tensor, and ultimately show the force on the sphere to be

$$\mathbf{F}_0 = -6\pi G a \mathbf{U}_0 \left(1 - a\Gamma_E - \frac{a^2\Gamma_E^2}{9}\right). \tag{2.195}$$

(2.3) **Correspondence Principle for oscillating spheres.** Show that the Correspondence Principle can be used to derive the stream functions for a sphere oscillating in an incompressible elastic solid (2.194) from the solutoin in an incompressible viscous liquid (2.93), and vice versa. Hint: You will need to compute $\sqrt{1/i}$, for which there are two choices, only one of which behaves well far from the sphere. Similarly, show that the force on a sphere oscillating in an elastic medium (2.195) can be obtained from the force on a sphere oscillating in a viscous liquid (2.100), and vice-versa.

(2.4) **Energy balance for sphere oscillating in elastic medium.** Using (2.195), show the force on a sphere of radius a in an elastic medium, undergoing a general displacement $\mathbf{U}(t)$ to be given by

$$\mathbf{F} = -6\pi Ga\mathbf{U} - \frac{\mathbf{V}}{c}6\pi Ga^2 - \frac{1}{2}M_a\ddot{\mathbf{U}}. \tag{2.196}$$

where $M_a = 4\pi a^3\rho_m/3$ is the equivalent mass of the elastic material occupied by the sphere.

Show that the power exerted by the sphere $P(t) = -\mathbf{F}\cdot\mathbf{V}$ on the material during an oscillatory displacement $\mathbf{U}_0 \sin\omega t$ is

$$P(t) = \frac{6\pi Ga^2}{c}U_0^2\omega^2\cos^2\omega t + \ldots \tag{2.197}$$

$$+\left(6\pi Ga\omega - \frac{M_f\omega^3}{2}\right)U_0^2\sin\omega t\cos\omega t. \tag{2.198}$$

Show that a sphere oscillating in an elastic medium exerts a time-averaged power on the medium,

$$\bar{P} = 3\pi\rho a^2 cU_0^2\omega^2. \tag{2.199}$$

Even in a purely elastic medium, the elastic energy of a displaced sphere is lost over time. Where does it go?

(2.5) **Correspondence Principle: Point forces in incompressible viscous and elastic media.** Evaluate Thomson's solution (2.126) for the elastic displacement field $\mathbf{u}$ around a point force $\mathbf{F}$, in the incompressible limit $K/G \to \infty$. Use the Correspondence Principle to replace G with $i\omega\eta$, and verify that the result is consistent with the Stokeslet (Oseen Tensor, eqn 2.82) flow $\mathbf{v}$ due to a point force.

(2.6) **Rotational oscillations in an elastic medium.** Consider a sphere of radius a executing oscillatory rotations with strain amplitude $\Theta(t) = \Theta_0 e^{i\omega t}$ about the $\theta = 0$ axis in an isotropic elastic medium, with shear modulus G and Poisson ratio ν. Show that the displacement field is given by

$$\mathbf{u}(t) = \Theta_0 \times \mathbf{r} \left(\frac{a}{r}\right)^3 \frac{1 + i\Gamma_E r}{1 + i\Gamma_E a} e^{i(\omega t - \Gamma_E (r-a))}, \tag{2.200}$$

where

$$\Gamma_E = \sqrt{\frac{\omega^2 \rho}{G}} = \frac{\omega}{c} \tag{2.201}$$

and where only outgoing shear waves are kept. Show that the torque on the sphere is given by

$$L_0 = 8\pi G a^3 \Theta_0 \left(1 - \frac{a^2 \Gamma_E^2}{3(1 + i\Gamma_E a)}\right), \tag{2.202}$$

to give a rotational spring constant

$$\kappa_R = 8\pi G a^3 \left(1 - \frac{a^2 \Gamma_E^2}{3(1 + i\Gamma_E a)}\right), \tag{2.203}$$

or resistance

$$\zeta_R^* = \frac{8\pi G a^3}{i\omega} \left(1 - \frac{a^2 \Gamma_E^2}{3(1 + i\Gamma_E a)}\right). \tag{2.204}$$

(2.7) **Rotational oscillations in a viscous fluid.** Consider a sphere of radius a executing oscillatory rotations with angular velocity $\Omega(t) = \Omega_0 e^{i\omega t}$ about the $\theta = 0$ axis in a Newtonian liquid with viscosity μ. Show that the velocity field is given by

$$\mathbf{v}(t) = \Omega_0 \times \mathbf{r} \left(\frac{a}{r}\right)^3 \frac{1 + \Gamma r}{1 + \Gamma a} e^{-\Gamma (r-a) + i\omega t} \tag{2.205}$$

where $\Gamma = (1 + i)/\lambda_V$, and where $\lambda_V = \sqrt{2\nu/\omega}$ is the oscillatory boundary-layer thickness. so that

$$\zeta_R^* = 8\pi \eta a^3 \left(1 - \frac{a^2 \Gamma^2}{3(1 + i\Gamma a)}\right), \tag{2.206}$$

(2.8) **Coupling mobility between two different-sized spheres.** Consider the leading-order approximation to the coupling mobility between two spheres of radii a_1 and a_2, located at $\mathbf{r}_1 = 0$ and $\mathbf{r}_2 = d\hat{\mathbf{x}}$, respectively. Start with the case where forces are parallel to the line of centers ($\mathbf{F}_i = F\hat{\mathbf{x}}$). Given a force $\mathbf{F}_1 = F\hat{\mathbf{x}}$ on sphere 1, what are the velocities $\mathbf{V}_1$ and $\mathbf{V}_2$ of spheres 1 and 2? Given a force $\mathbf{F}_2 = F\hat{\mathbf{x}}$ on sphere 2, what are the velocities $\mathbf{V}_1$ and $\mathbf{V}_2$ of spheres 1 and 2? Construct the mobility tensor

$$\begin{pmatrix} \mathbf{V}_1 \\ \mathbf{V}_2 \end{pmatrix} = \begin{pmatrix} \mathbf{b}^{11} & \mathbf{b}^{12} \\ \mathbf{b}^{21} & \mathbf{b}^{22} \end{pmatrix} \cdot \begin{pmatrix} \mathbf{F}_1 \\ \mathbf{F}_2 \end{pmatrix}, \tag{2.207}$$

for different-sized spheres. What are the two eigenmodes of this system? What happens when $a_1 \gg a_2$?

(2.9) **Coupling mobility between two identical spheres, forced perpendicular to line of centers.** Compute the leading-order coupling mobility $\mathbf{b}_{21}^{\perp}$ for two identical spheres of radius a, separated by $\mathbf{d} = d\hat{\mathbf{x}}$. Verify (2.149).

(2.10) **Coupling resistance between two identical spheres.** Now, consider the the leading-order approximation to the coupling *resistance* between two spheres of radius a, located at $\mathbf{r}_1 = 0$ and $\mathbf{r}_2 = d\hat{\mathbf{x}}$, respectively. Start with the case where velocities are parallel to the line of centers ($\mathbf{V}_i = V\hat{\mathbf{x}}$). Given a force $\mathbf{V}_1 = V\hat{\mathbf{x}}$ on sphere 1, what are the forces $\mathbf{F}_1$ and $\mathbf{F}_2$ on spheres 1 and 2? Given a velocity $\mathbf{V}_2 = F\hat{\mathbf{x}}$ on sphere 2, what are the forces $\mathbf{F}_1$ and $\mathbf{F}_2$ of spheres 1 and 2? Construct the resistance tensor

$$\begin{pmatrix} \mathbf{F}_1 \\ \mathbf{F}_2 \end{pmatrix} = \begin{pmatrix} \xi^{11} & \xi^{12} \\ \xi^{21} & \xi^{22} \end{pmatrix} \cdot \begin{pmatrix} \mathbf{V}_1 \\ \mathbf{V}_2 \end{pmatrix}. \tag{2.208}$$

Invert this tensor to find the mobility tensor,

$$\mathbf{b} = \boldsymbol{\xi}^{-1}, \tag{2.209}$$

and show it agrees with (2.145).

(2.11) **Sphere near a free surface.** Section 2.6.4 computed the hydrodynamic mobility of a sphere of radius a located a distance h from a planar, no-slip wall (*e.g.*, a glass slide). Now, compute the hydrodynamic mobility of a sphere in the vicinity of a free surface (*e.g., a liquid-gas interface*), where a no-stress condition ($\tau_{xz} = 0$) holds at the wall. Show that "wall flow"

for a sphere forced towards the wall can be expressed simply by a Stokeslet,

$$\mathbf{u}_w^{\perp} = -\mathbf{G}^{St}(\mathbf{r} + h\hat{\mathbf{z}}) \cdot \mathbf{F}^{\perp}\hat{\mathbf{z}} \tag{2.210}$$

$$\mathbf{u}_w^{\parallel} = \mathbf{G}^{St}(\mathbf{r} + h\hat{\mathbf{z}}) \cdot \mathbf{F}^{\parallel}\hat{\mathbf{x}} \tag{2.211}$$

located behind the wall at the image location $\mathbf{r}_i = -h\hat{\mathbf{z}}$, similarly directed for parallel forces $\mathbf{F}_{\parallel}$ and oppositely directed for perpendicular forces $\mathbf{F}_{\perp}$. That is, show that

$$\mathbf{u}^{\perp} = \left[\mathbf{G}^{St}(\mathbf{r} - h\hat{\mathbf{z}}) - \mathbf{G}^{St}(\mathbf{r} + h\hat{\mathbf{z}})\right] \cdot \mathbf{F}^{\perp} \tag{2.212}$$

$$\mathbf{u}^{\parallel} = \left[\mathbf{G}^{St}(\mathbf{r} - h\hat{\mathbf{z}}) + \mathbf{G}^{St}(\mathbf{r} + h\hat{\mathbf{z}})\right] \cdot \mathbf{F}^{\parallel} \tag{2.213}$$

obeys the no-flux and no-stress conditions

$$\left.\frac{\partial u_x}{\partial z}\right|_{z=0} = 0 \tag{2.214}$$

$$\left.\frac{\partial u_y}{\partial z}\right|_{z=0} = 0 \tag{2.215}$$

$$u_z(x, y, z = 0) = 0. \tag{2.216}$$

Given this, show that the leading-order correction to the sphere's mobility is given by

$$b^{\parallel} = \frac{1}{6\pi\eta a}\left(1 + \frac{3a}{8h}\right) \tag{2.217}$$

$$b^{\perp} = \frac{1}{6\pi\eta a}\left(1 - \frac{3a}{4h}\right). \tag{2.218}$$